Deformation Analysis of Ground Foundation

—— Usage and theory of DACSAR

Visiting scholar in RCUSS
of Kobe university
Zhang Xiangxia

2008-03-04

DACSAR stands for

Deformation Analysis Considering Stress Anisotropy and Reorientation

DACSAR Soil and water coupled Elasto-viscoplastic F.E. code

– open to the public –

地盤工学会全国大会
1984-2003
有効応力解析416件
内，使用ソフト名明記117件中
DACSAR:101件(86%)
他に，CRISP:4，FUTO:3
ABAQUS:2，SIGNAS:2など

MOMIS: A database for the numerical modeling of embankments on soft soils and the comparison between computational

The figure shows the result of investigation by LCPC. DACSAR is one of the most popular program to predict the soil behavior.

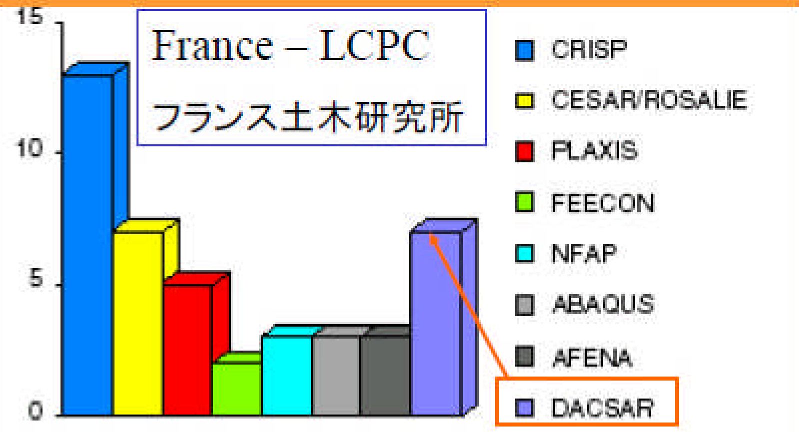

Fig. 6 - Numbers of citations of finite element computation software found in MOMIS database references (references to CESAR-LCPC and ROSALIE-LCPC have been combined in this figure).

Bulletin Laboratoires des Ponts et Chaussees, 232, pp.45-60, 2001

DACSARs:

- DACSAR (DACSAR-original)

  Open to the public
- DACSAR-MC (DACSAR-updated)

  * EC/LC model is incorporated;
  * Subloading surface;
  * Macro element is incorporated;

  Open to the public
- DACSAR-3D (3-Dimensional version of DACSAR)

  Not open to the public
- DACSAR-F (finite deformation version of DACSAR)

  Soil/water coupled elasto-plastic FE based on incremental finite deformation theory

  Not open to the public
- DACSAR-U

  Unsaturated soil/water coupled elasto-plastic FE

  Not open to the public
- DACSAR-D

  Dynamic soil/water coupled elasto-plastic FE

  Not open to the public

CONTENTS

CONTENTS

CONTENTS

1-DESCRIPTION of DACSAR

- **Introduction**
- **Origination of report**
- **Program overview**

- **Program overview for DACSAR-MC**

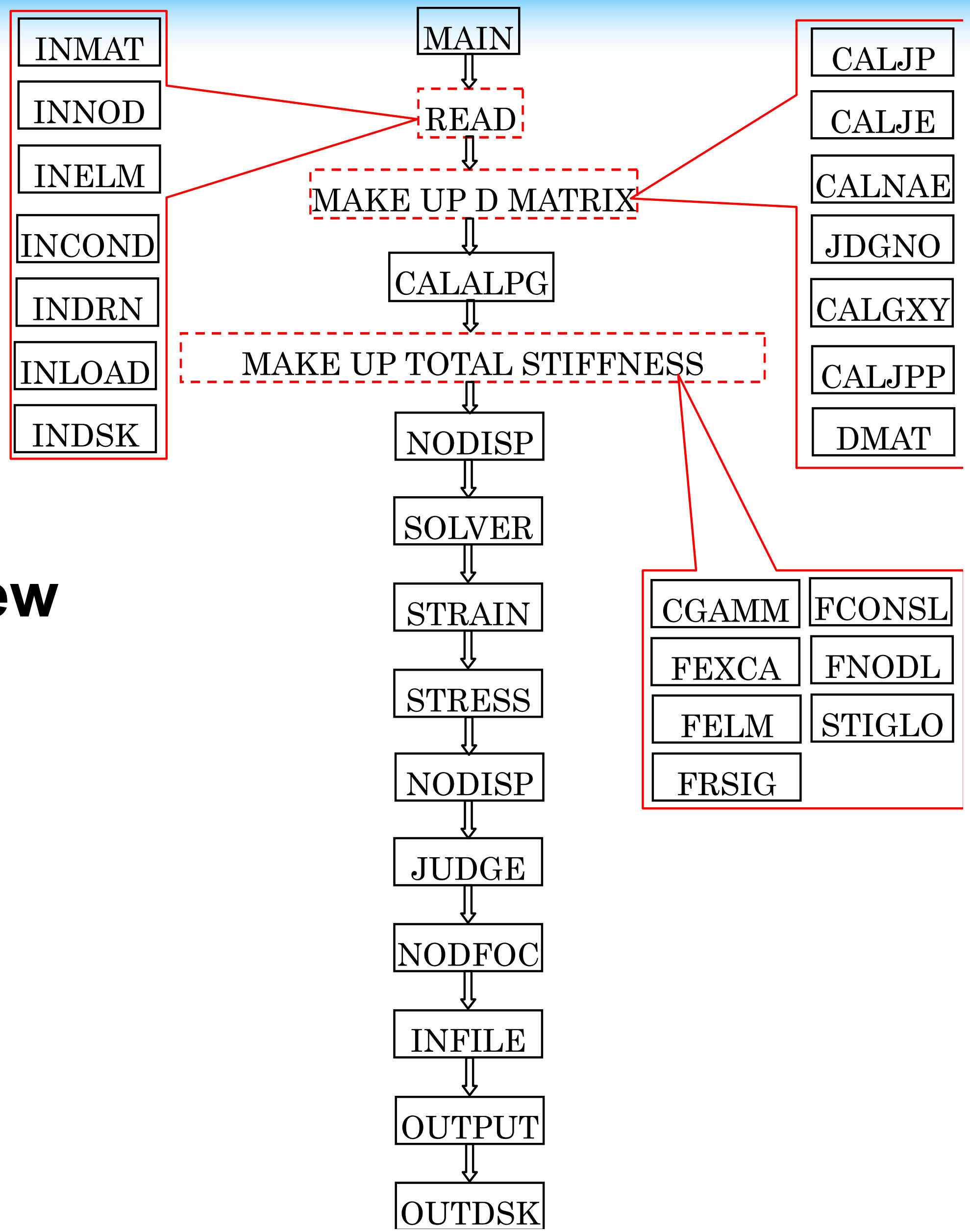

CONTENTS

2-Details of theories used in DACSAR

1. **Constitutive models employed in DACSAR**
2. **Singular point on the yielding surface (SO)**
3. **Yielding Judgment**
4. **Metastability (SO-EP)**
5. **Functions**
6. **Macro element proposed by Sekiguchi et al.**
7. **Bar, Beam, Joint, Shell element etc.**

1.Constitutive models employed in DACSAR

1.1 Theoretical explanation

1.2 Demonstration

1.1 Theoretical explanation

MT	Element type
0	Elasto-(visco)plastic plane element
1	Linearly elastic plain element
2	Linearly elastic Beam element
3	Linearly elastic Bar element
4	Elastic perfectly plastic Joint element
5	Linearly plastic Shell element
6	Drucker-Prager plane element
7	Hyperbolic plane element
8	Modified Cam-Clay model
9	EC model element
10	LC model element

Constitutive models are discussed here

Constitutive models used in DACSAR

MT	Model type
MT=0	Sekiguchi-Ohta model, includs (1) SO-EP model (2) SO-EVP model; (3) SO-EP with subloading surface model(SOSS model)
MT=1	Linear elastic materials
MT=6	Drucker-Prager model
MT=7	Hyperbolic materials
MT=8	Modified Cam-Clay model
MT=9	EC model (Exponential contractancy model), includs (1) EC-EP model (2) EC-EVP model (3) EC-EP with subloading surface model(SOSS model)
MT=10	LC model (Logarithmic contractancy model), includs (1) LC-EP model (2) LC-EVP model (3) LC-EP with subloading surface model(SOSS model)

MT=0, Sekiguchi-Ohta model

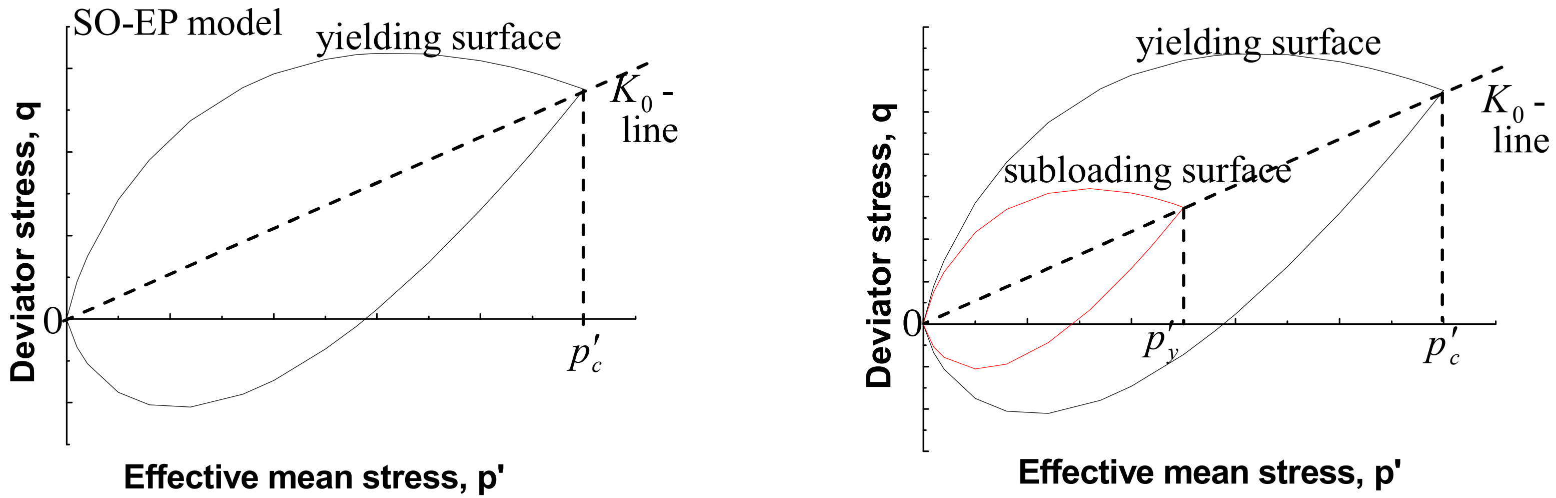

(a) Yield surface of SO-E(V)P model **(b) Sketch of subloading surface**

Fig1.1 Yield surface of SO model

MT=6, Drucker-Prager model
MT=8, Modified Cam-Clay model

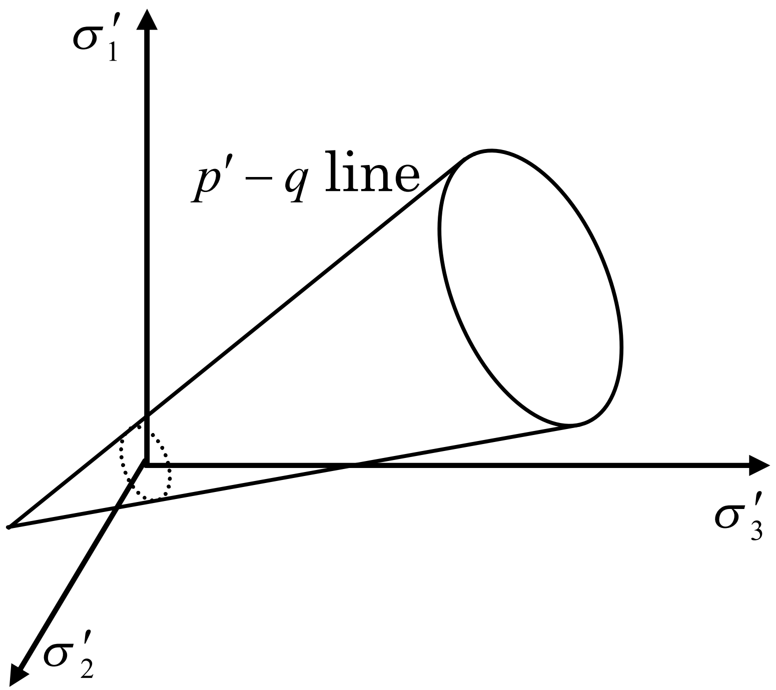

Fig1.2 Yield surface of DP model in principal stress space

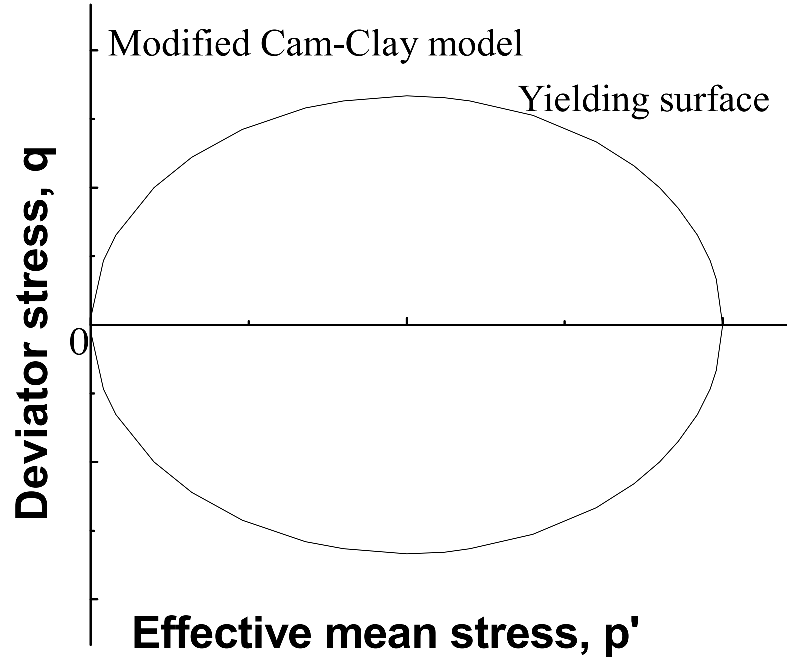

Fig1.3 Yield surface of Modified Cam-Clay model

MT=9, EC model (Exponential contractancy model)
MT=10, LC model (Logarithmic contractancy model)

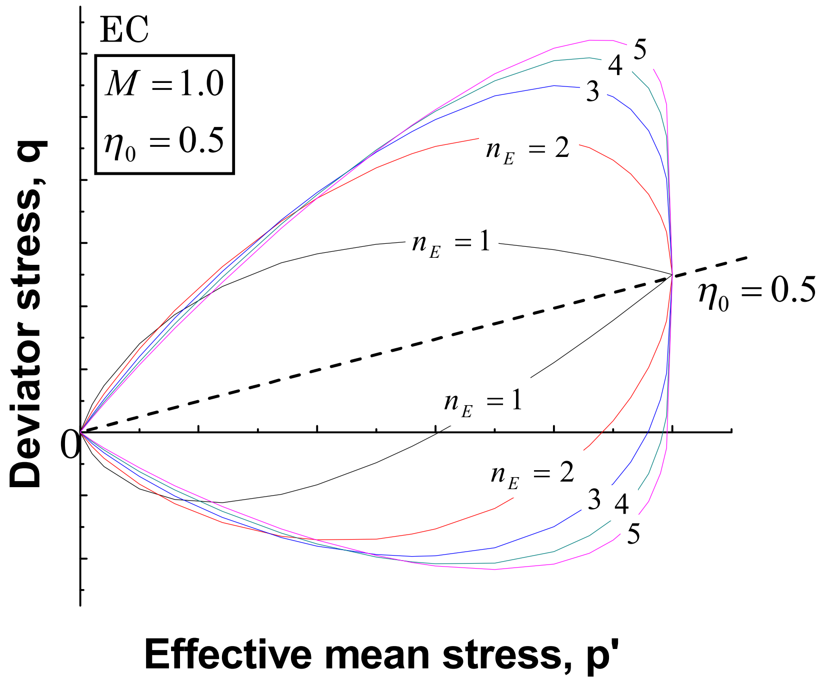

Fig1.4 Yield surface of EC model

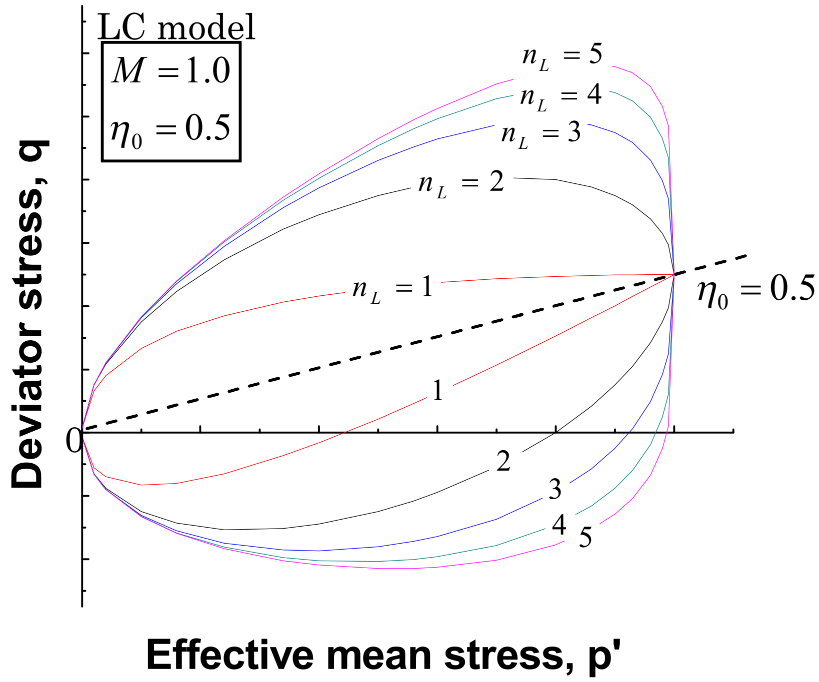

Fig1.5 Yield surface of LC model

1.2 Demonstration

Case 0 for 1D consolidation for OCR=1

1D consolidation for OCR=1	Linear model	SO model	DP model	EC model	LC model
	case 0				

Value of parameters

Lame's constant		Permeability
$\tilde{\lambda}\left(kg/cm^2\right)$	$\tilde{\mu}\left(kg/cm^2\right)$	$k\left(cm/\min\right)$
13.661	6.805	$6.0*10^{-6}$

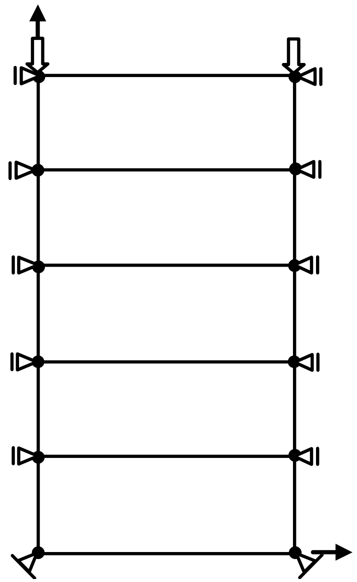

Fig1.6 Boundary condition for Case 0

1.2 Demonstration

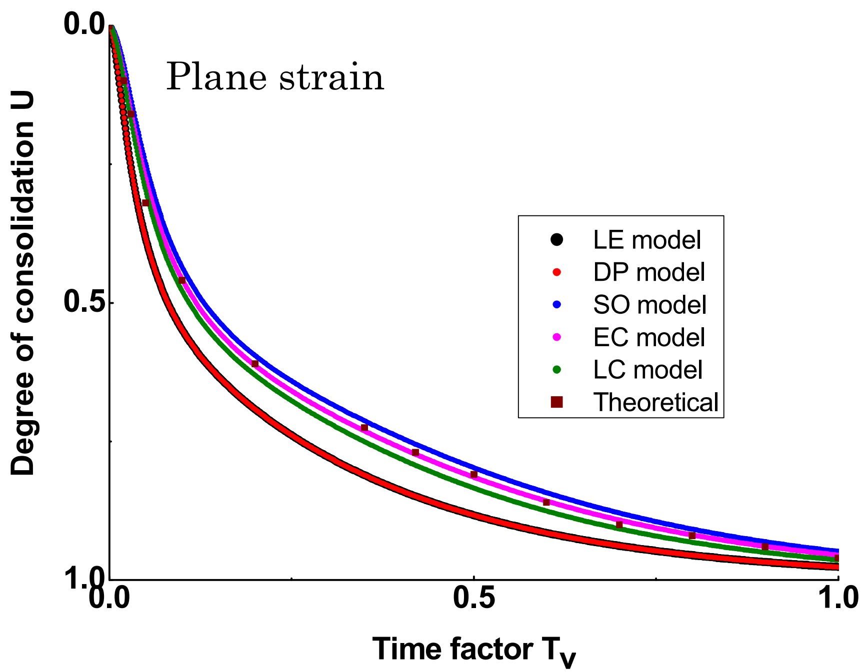

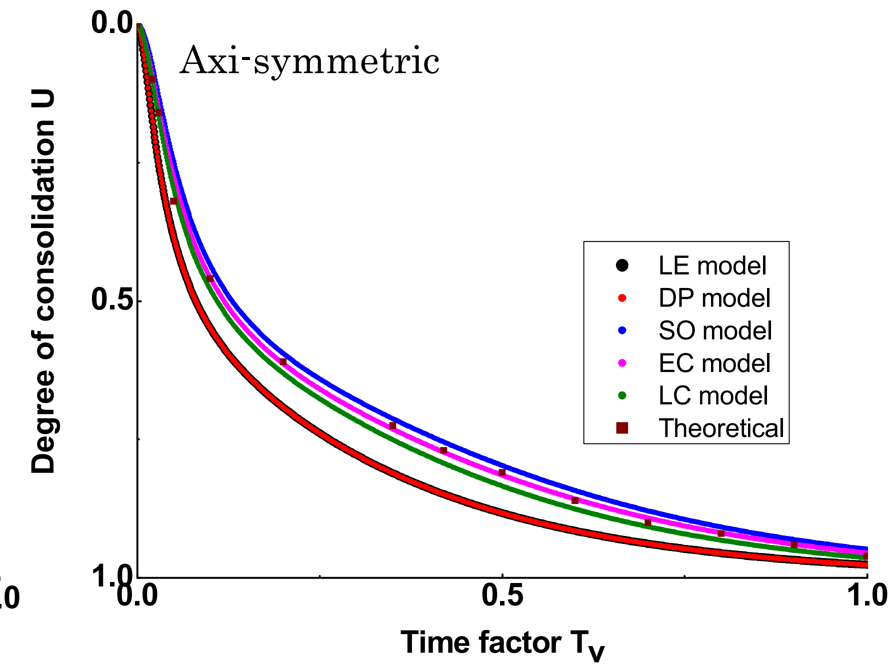

Fig1.7(a) Relationship between degree of consolidation and time factor

1.2 Demonstration

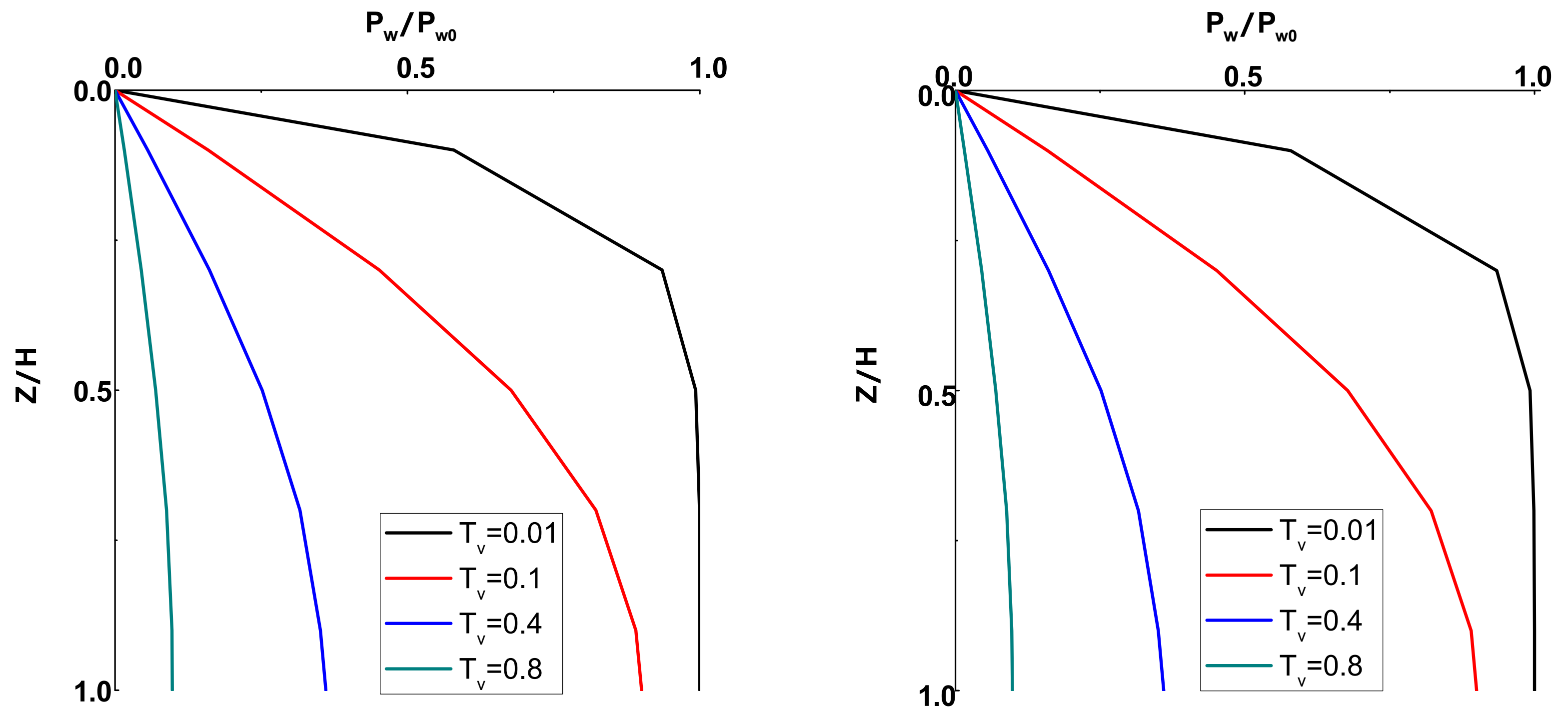

Fig1.7(b) Consolidation Isochrone for Case 0 by using linear elastic model

1.2 Demonstration

Case (1-1)～(3-19) for the application of different constitutive models with different value of OCR and different drainage condition

OCR	Drainage condition	SO- model			EC-model			LC-model		
		EP	EVP	SS	EP	EVP	SS	EP	EVP	SS
1	Undrained	(1-1)	(1-2)	(1-3)	(1-4)	(1-5)	(1-6)	(1-7)	(1-8)	(1-9)
	Fully draind	(1-11)	(1-12)	(1-13)	(1-14)	(1-15)	(1-16)	(1-17)	(1-18)	(1-19)
2	Undrained	(2-1)	(2-2)	(2-3)	(2-4)	(2-5)	(2-6)	(2-7)	(2-8)	(2-9)
	Fully draind	(2-11)	(2-12)	(2-13)	(2-14)	(2-15)	(2-16)	(2-17)	(2-18)	(2-19)
20	Undrained	(3-1)	(3-2)	(3-3)	(3-4)	(3-5)	(3-6)	(3-7)	(3-8)	(3-9)
	Fully draind	(3-11)	(3-12)	(3-13)	(3-14)	(3-15)	(3-16)	(3-17)	(3-18)	(3-19)

Three types of tests including plane strain shear, axisymmetric shear and direct shear

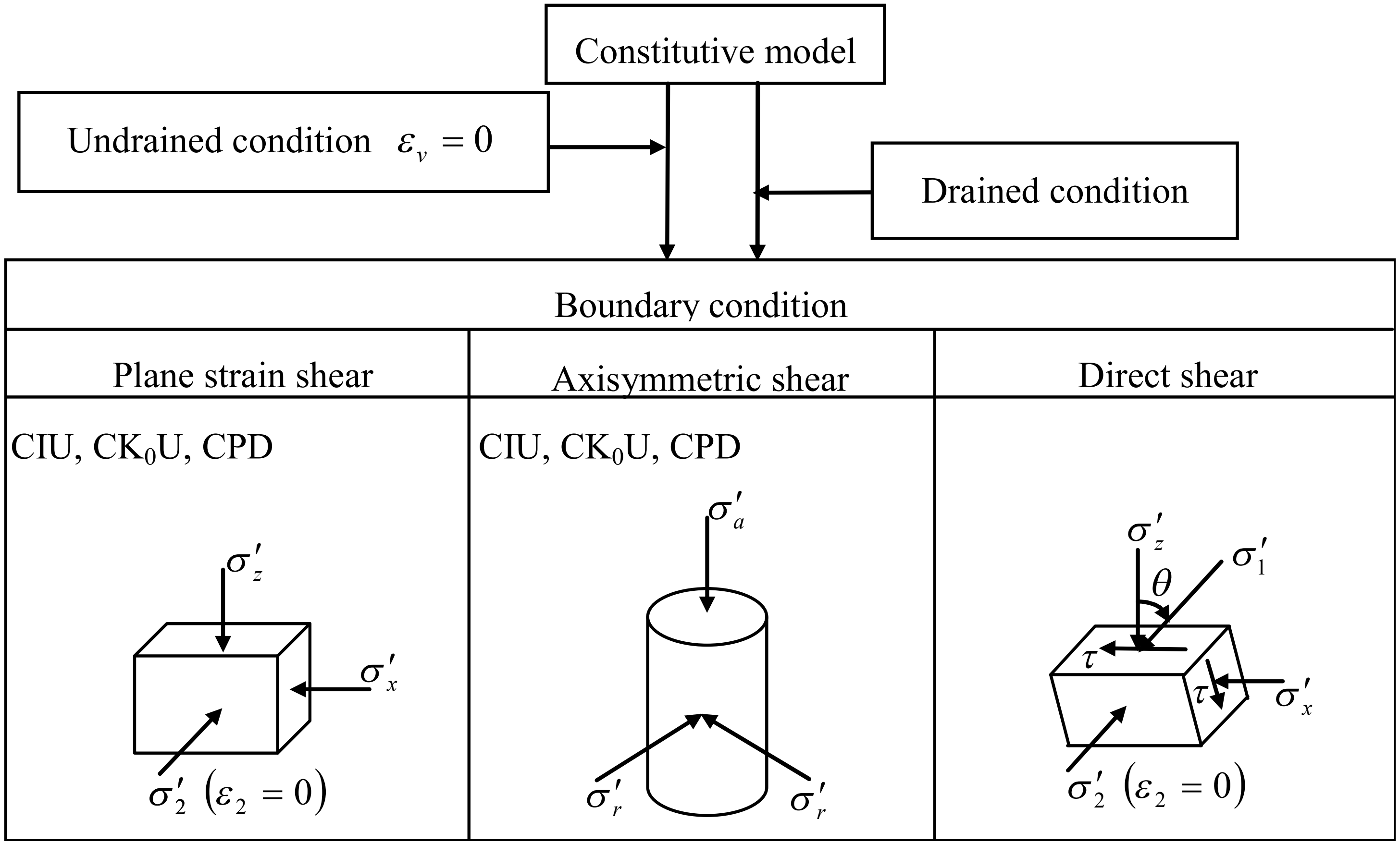

Fig1.8 Three types of tests

Effect of corresponding parameter to some model is considered

	Elasto-plastic	Elasto-viscoplastic	Subloading surface
SO model		$\dot{\varepsilon}_z(\dot{\varepsilon}_a) = 0.1\%/\min$ $\dot{\varepsilon}_z(\dot{\varepsilon}_a) = 0.01\%/\min$	$m = 1$ $m = 10$ $m = 100$
EC model	$n_E = 1.0$ (SO model) $n_E = 1.5$ $n_E = 2.0$		
LC model	$n_L = 1.5$ $n_L = 2.0$ $n_L = 2.5$		

Input parameters

D	0.076	$\sigma'_{v0}(\mathrm{kg/cm^2})$	1.0
Λ	0.549	$\sigma'_{vi}(\mathrm{kg/cm^2})$	1.0
M	0.961	$\dot{v}_0(1/\mathrm{min})$	0.001%
ν'	0.394	λ	0.245
K_0	0.65	K_i	0.65
α	0.00667	e_0	0. 84

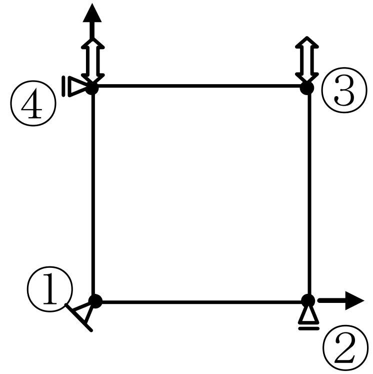

Fig.1.9 One element F.E. mesh and boundary condition

Case1-1 SO-EP model for undrained condition with OCR=1

(Same with Case1-3 SO-SS model)

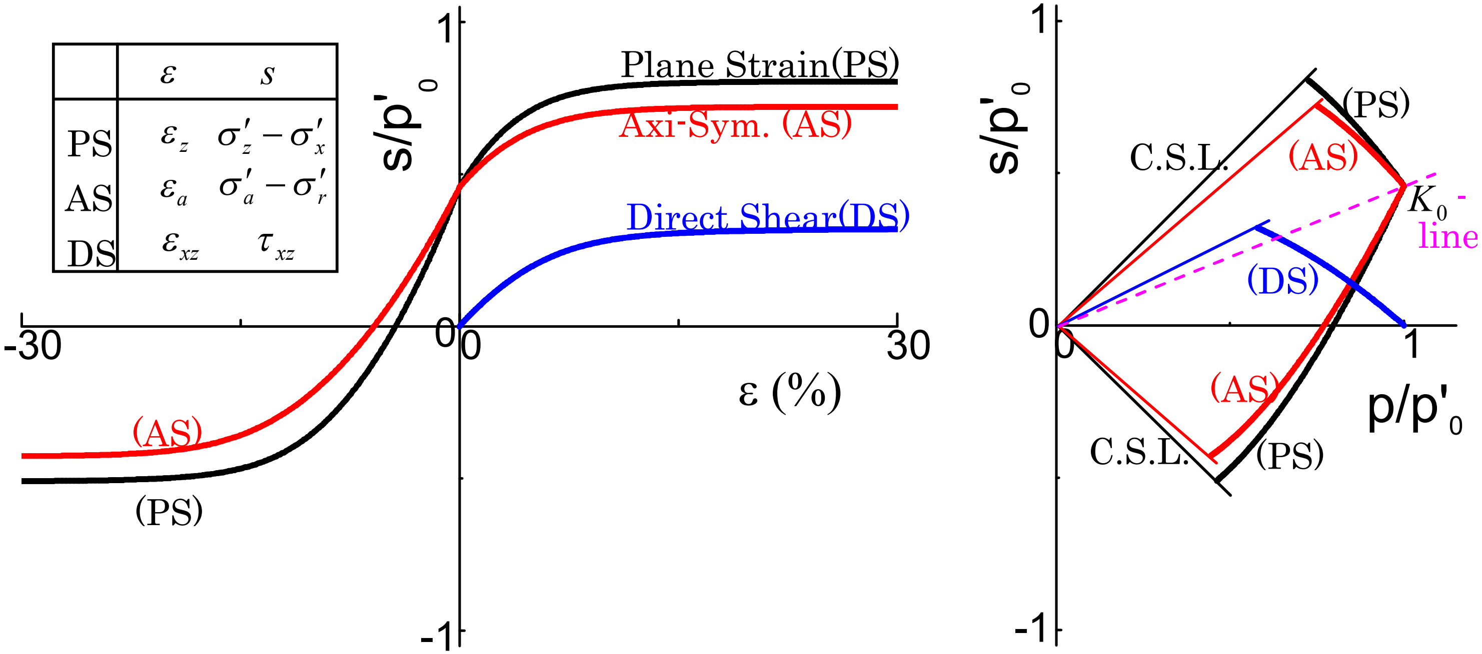

Fig1.10 Stress-strain relation and effective stress path

Case1-2 SO-EVP model for undrained condition with OCR=1

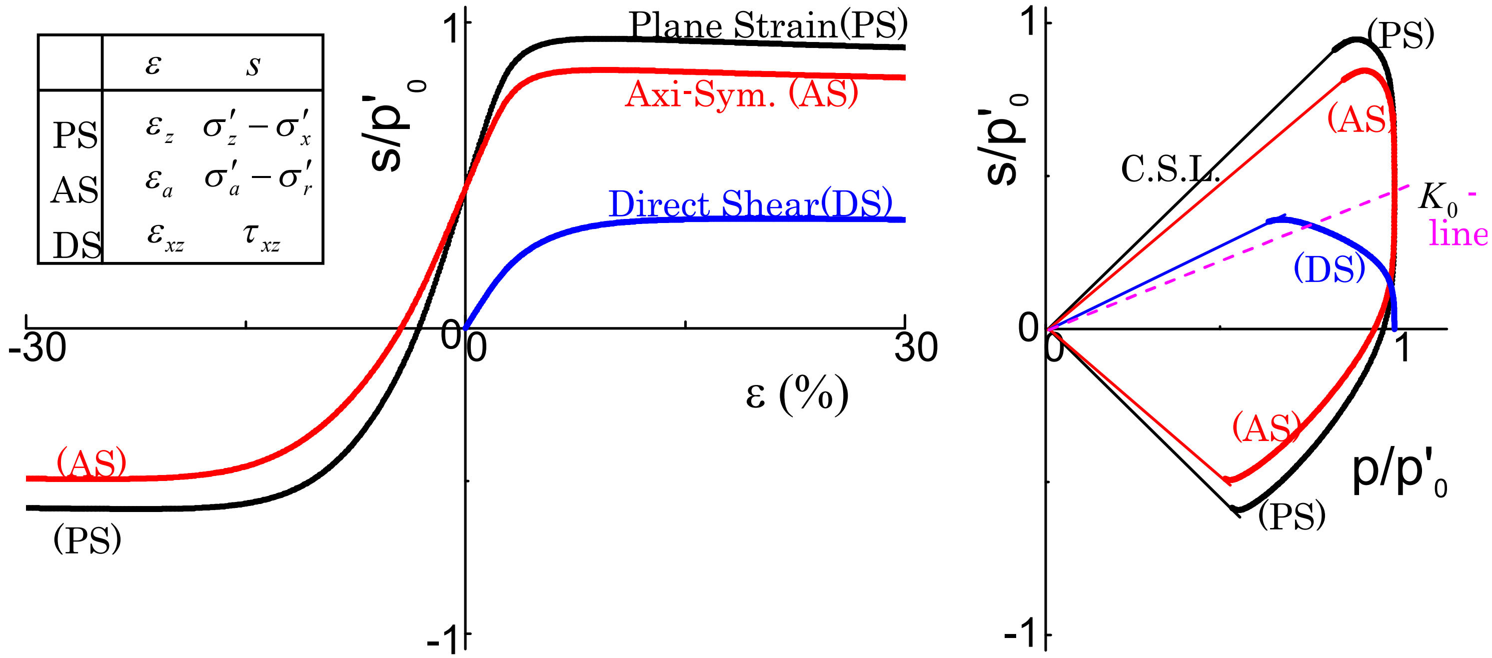

$\dot{\varepsilon}_z(\dot{\varepsilon}_a) = 0.1\%/\min$

Fig1.11 Stress-strain relation and effective stress path

Case1-4 EC-EP model for undrained condition with OCR=1

(Same with Case1-6 EC-SS model)

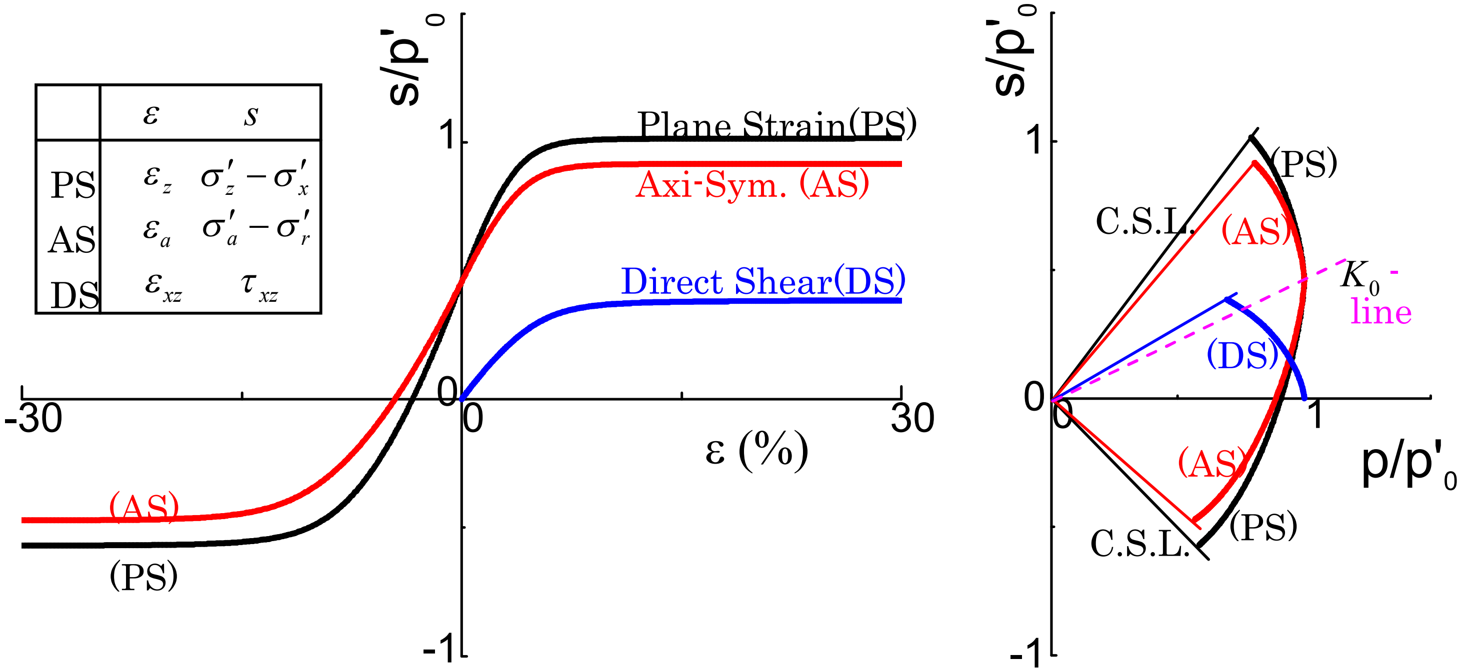

$n_E = 1.5$

Fig1.12 Stress-strain relation and effective stress path

Case1-5 EC-EVP model for undrained condition with OCR=1

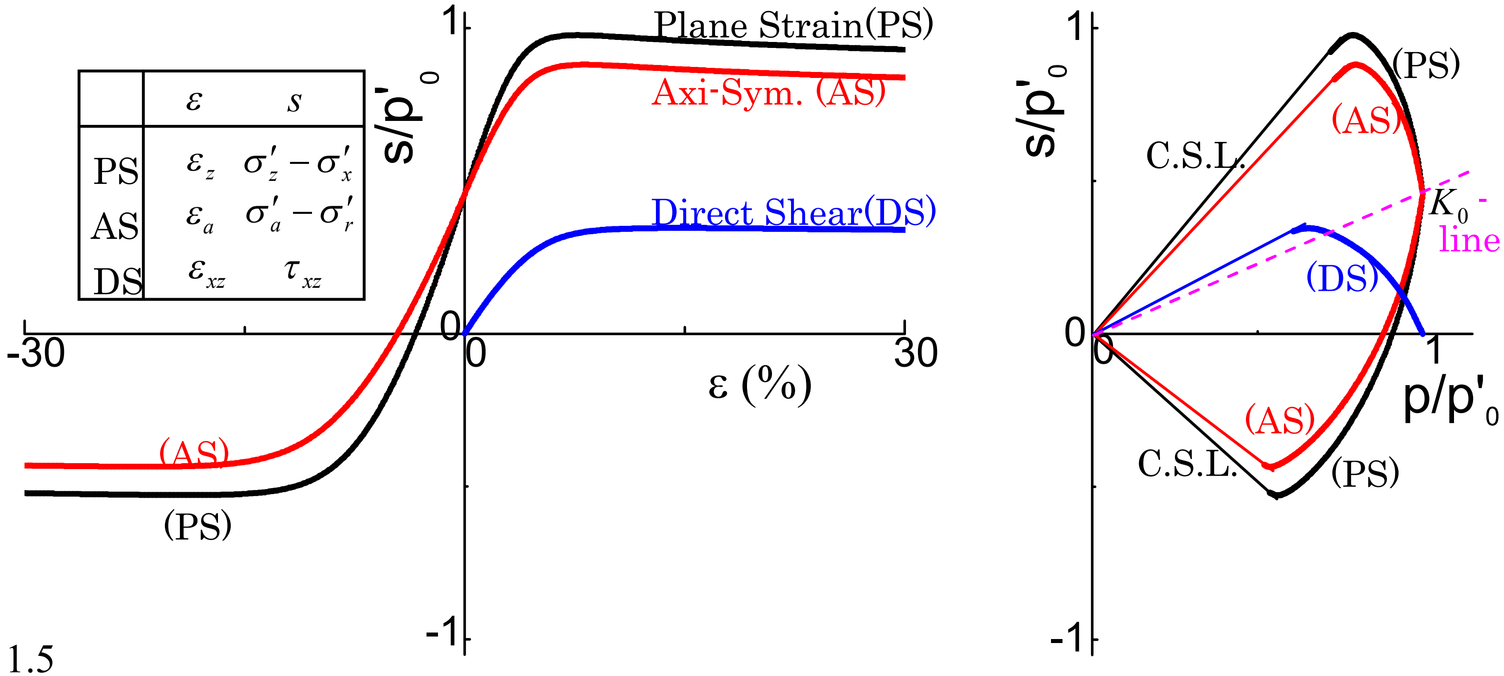

$n_E = 1.5$

$\dot{\varepsilon}_z(\dot{\varepsilon}_a) = 0.1\%/\min$

Fig1.13 Stress-strain relation and effective stress path

Case1-7 LC-EP model for undrained condition with OCR=1

(Same with Case1-9 LC-SS model)

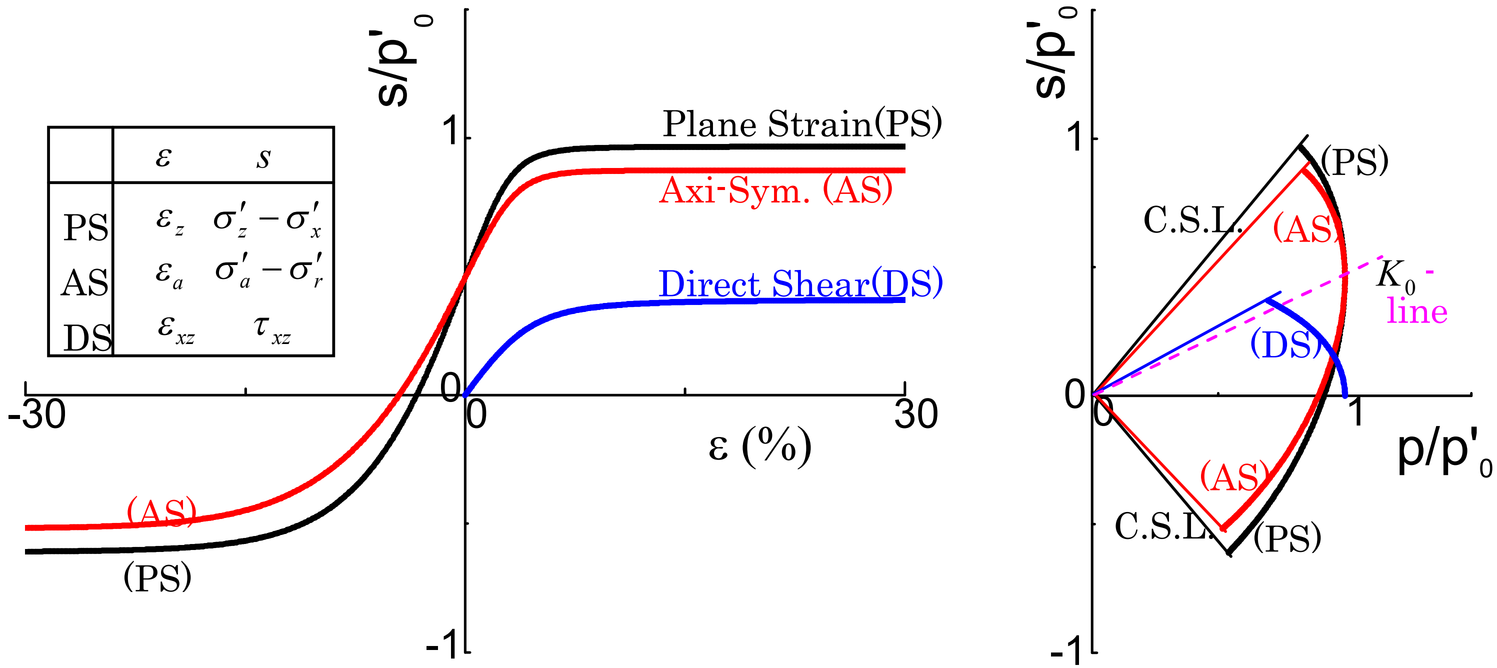

$n_L = 2$

Fig1.14 Stress-strain relation and effective stress path

Case1-8 LC-EVP model for undrained condition with OCR=1

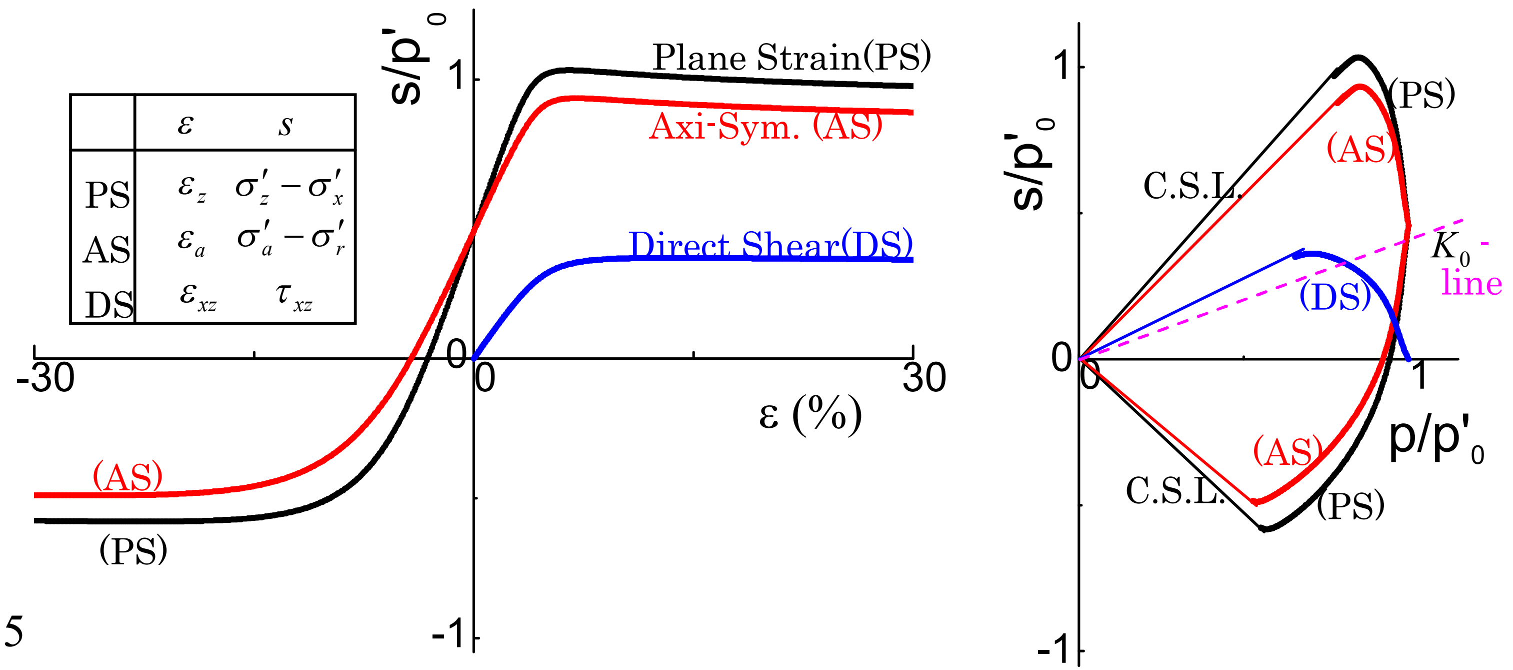

$n_L = 2.5$

$\dot{\varepsilon}_z(\dot{\varepsilon}_a) = 0.1\%/\mathrm{min}$

Fig1.15 Stress-strain relation and effective stress path

Case2-1 SO-EP model for undrained condition with OCR=2

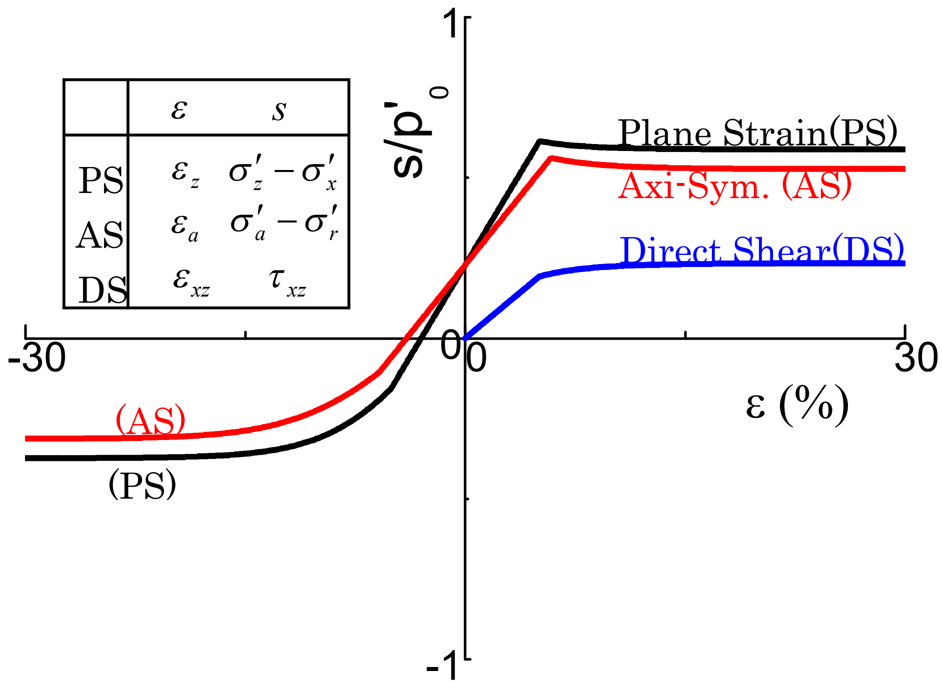

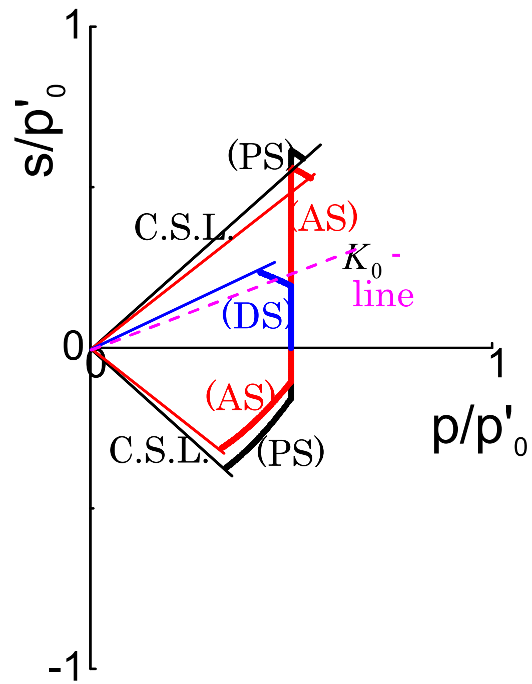

Fig1.16 Stress-strain relation and effective stress path

Case3-1 SO-EP model for undrained condition with OCR=20

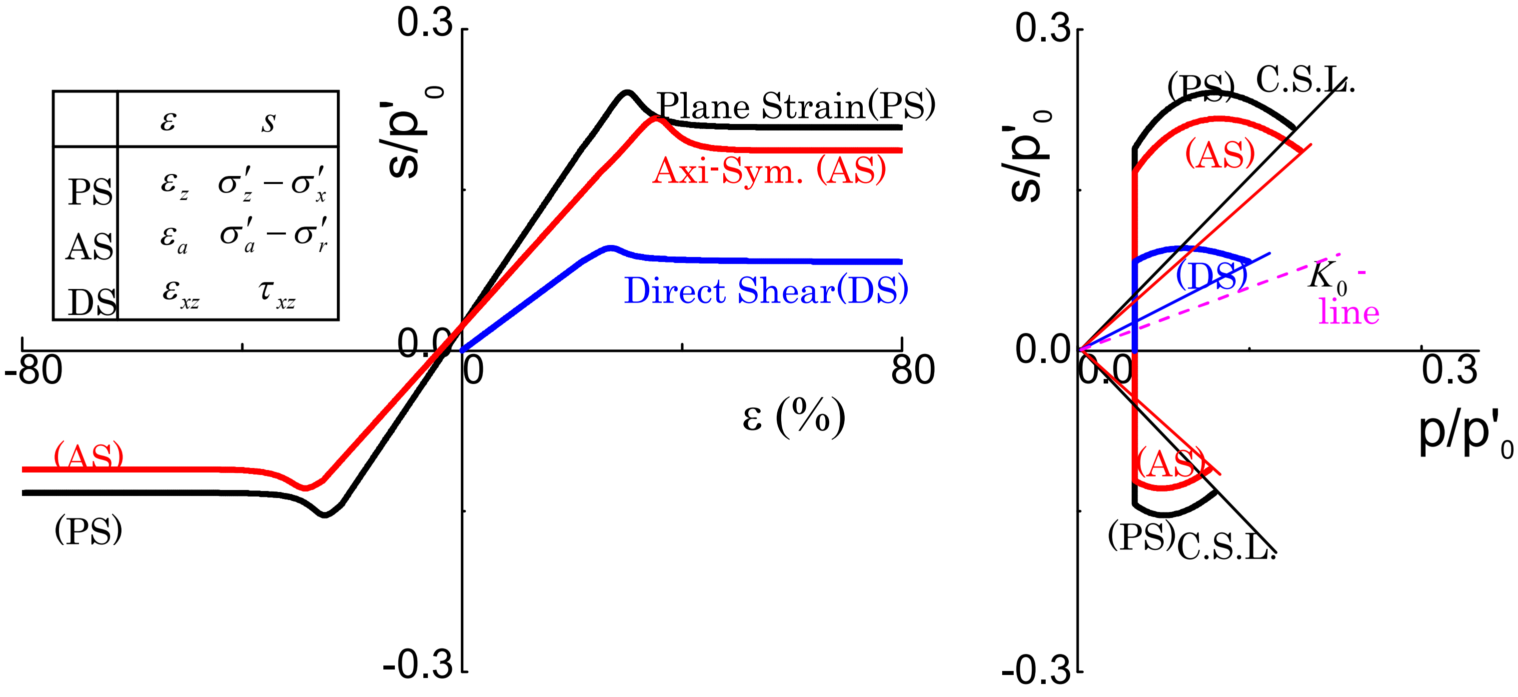

Fig1.17 Stress-strain relation and effective stress path

Case3-3 SO-SS model for undrained condition with OCR=20

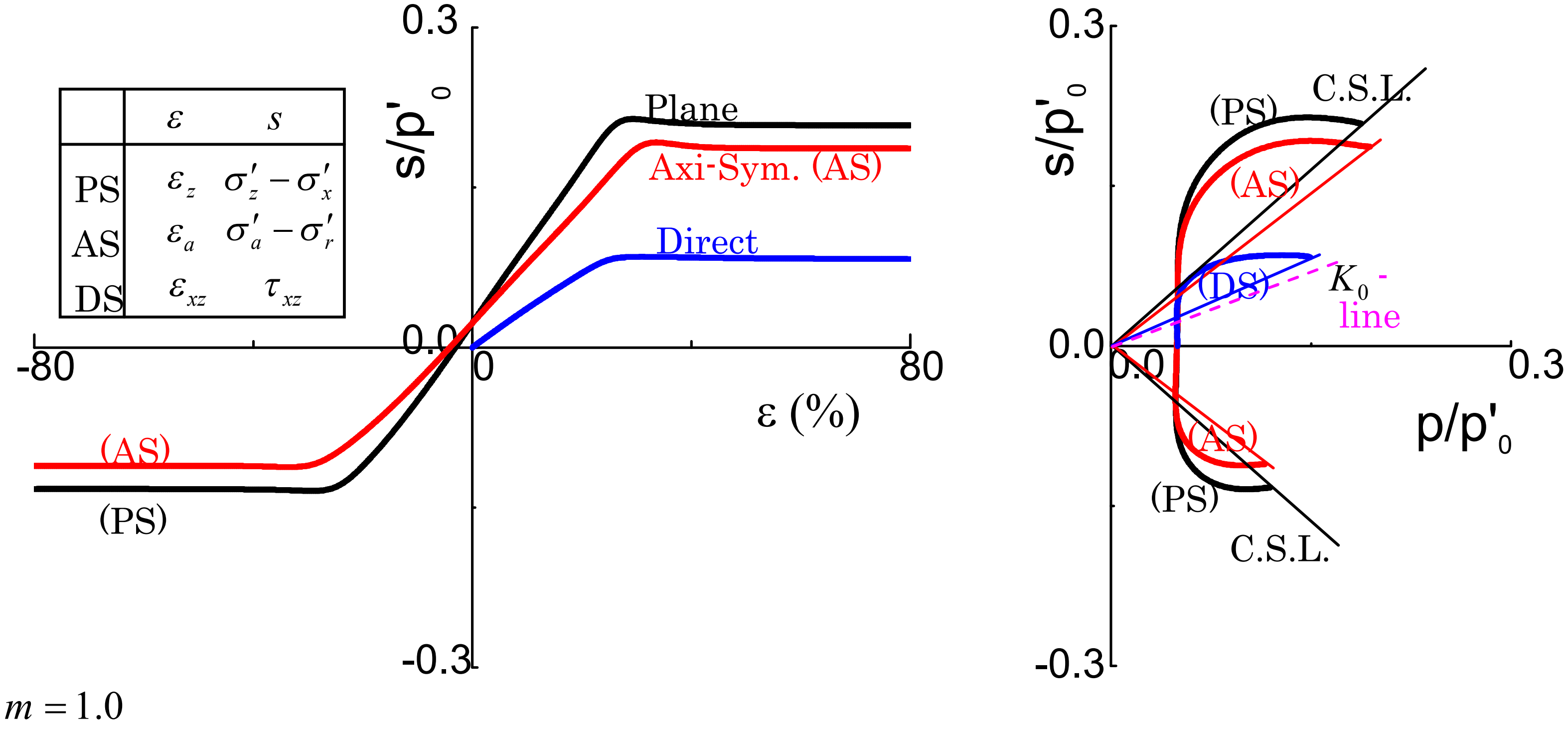

Fig1.18 Stress-strain relation and effective stress path

Case3-3 SO-SS model for undrained condition with OCR=20

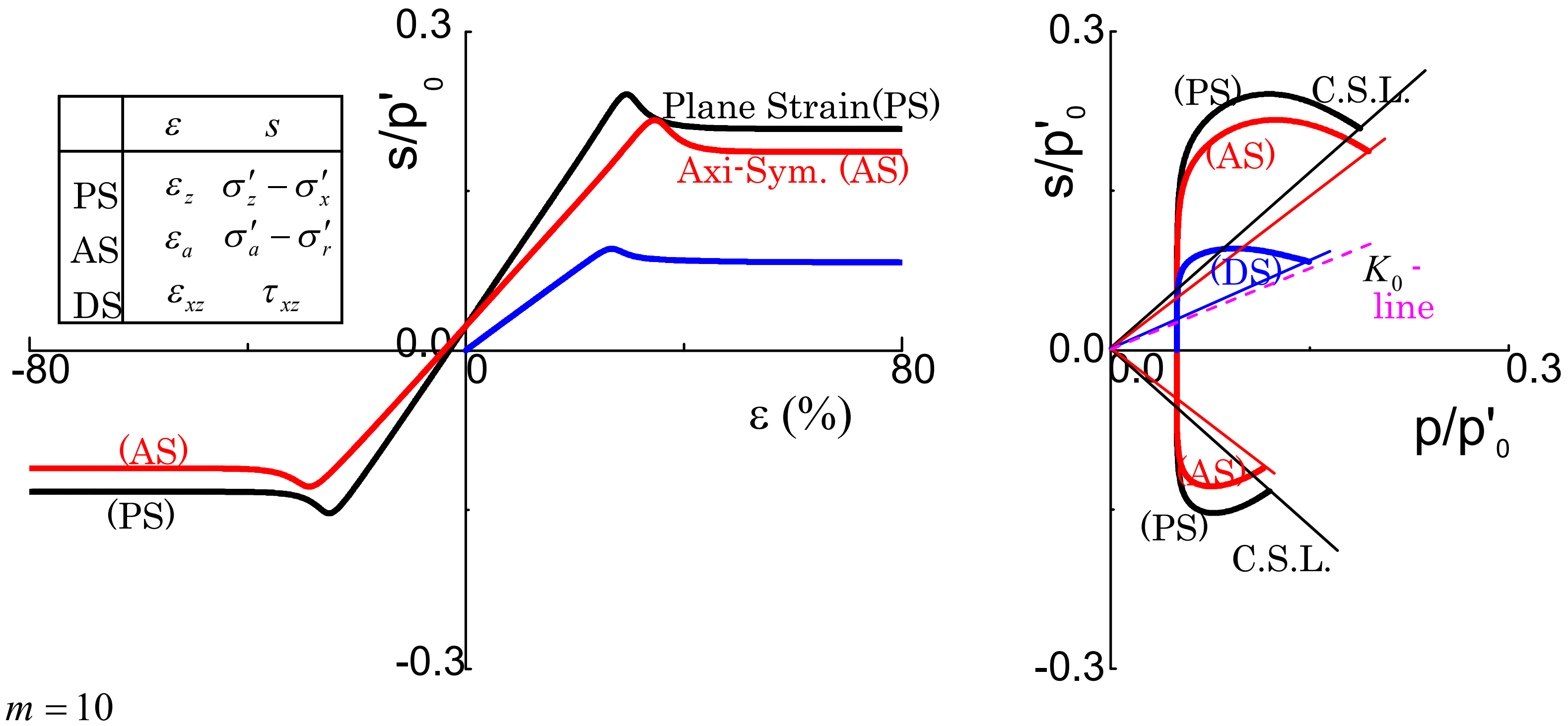

Fig1.19 Stress-strain relation and effective stress path

Case3-3 SO-SS model for undrained condition with OCR=20

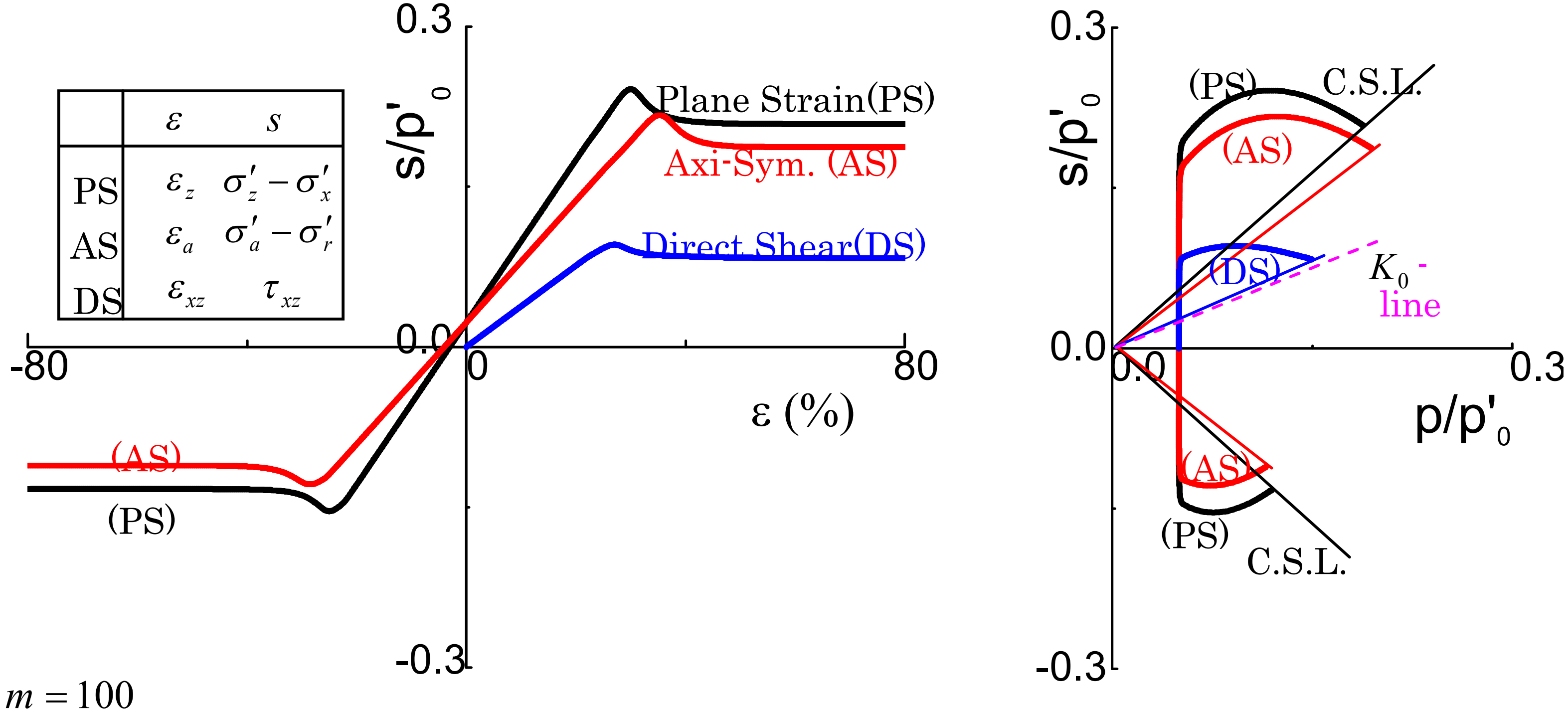

Fig1.20 Stress-strain relation and effective stress path

2-Details of theories used in DACSAR

1. **Constitutive models employed in DACSAR**
2. **Singular point on the yielding surface (SO)**
3. **Yielding Judgment**
4. **Metastability (SO-EP)**
5. **Functions**
6. **Macro element proposed by Sekiguchi et al.**
7. **Bar, Beam, shell element etc.**

2. Singular point on the yielding surface

(Takeyama,2007, Doctoral dissertation)

2.1 Explanation of theoretical treatment

2.2 Demonstration

Associated flow rule : $$\dot{\boldsymbol{\varepsilon}}^p = \dot{\gamma}\frac{\partial f}{\partial \boldsymbol{\sigma}'}$$

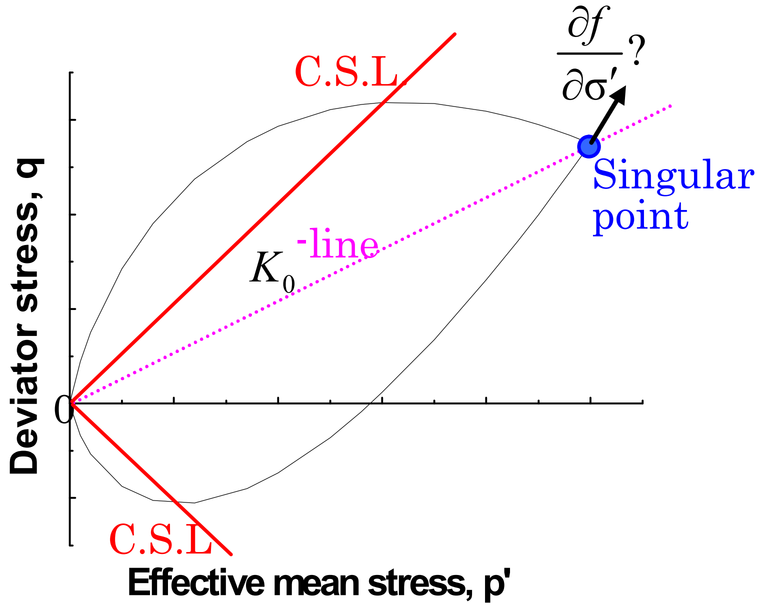

Fig 2.1 Singular point on the yield surface of SO model

Governing function for the singular point

Koiter's associated flow rule: $\dot{\varepsilon}^{\mathrm{p}} = \dot{\gamma}_1 \partial_{\sigma'} f_1 + \dot{\gamma}_2 \partial_{\sigma'} f_2$

Consistency condition: $\dot{f}_1 = 0$, $\dot{f}_2 = 0$

Yield function:

$$f_1(\sigma', \varepsilon_v^{\mathrm{p}}) = MD \ln \frac{p'}{p'_0} + D\sqrt{\frac{3}{2}} \frac{(\bar{\mathrm{s}} : \bar{\mathrm{n}}_v)}{p'} - \varepsilon_v^{\mathrm{p}} = 0$$

$$f_2(\sigma', \varepsilon_v^{\mathrm{p}}) = MD \ln \frac{p'}{p'_0} - D\sqrt{\frac{3}{2}} \frac{(\bar{\mathrm{s}} : \bar{\mathrm{n}}_v)}{p'} - \varepsilon_v^{\mathrm{p}} = 0$$

Plastic proportional coefficient:

$$\begin{Bmatrix} \dot{\gamma}_1 \\ \dot{\gamma}_2 \end{Bmatrix} = \frac{1}{\det X} \begin{bmatrix} X_{22} & -X_{12} \\ -X_{21} & X_{11} \end{bmatrix} \begin{Bmatrix} L_1 \\ L_2 \end{Bmatrix}$$

where, $\det X = X_{11} X_{22} - X_{12} X_{21}$

$$X_{11} = \frac{D^2}{p'^2}\left(\beta_1{}^2 K + 3G + \frac{p'}{D}\beta_1\right), \quad X_{12} = \frac{D^2}{p'^2}\left(\beta_1 \beta_2 K - 3G + \frac{p'}{D}\beta_2\right)$$

$$X_{21} = \frac{D^2}{p'^2}\left(\beta_1 \beta_2 K - 3G + \frac{p'}{D}\beta_1\right), \quad X_{22} = \frac{D^2}{p'^2}\left(\beta_2{}^2 K + 3G + \frac{p'}{D}\beta_2\right)$$

$$\beta_1 = \mathrm{M}\text{-}\sqrt{\frac{3}{2}}(\eta_0 : \bar{\mathrm{n}}_v), \; \beta_2 = \mathrm{M}\text{-}\sqrt{\frac{3}{2}}(\eta_0 : \bar{\mathrm{n}}_v), \; \bar{\mathrm{n}}_v = \frac{(1-\Lambda)K\dot{\varepsilon}_v \eta_0 - 2G\dot{\varepsilon}_d}{\left\|(1-\Lambda)K\dot{\varepsilon}_v \eta_0 - 2G\dot{\varepsilon}_d\right\|}$$

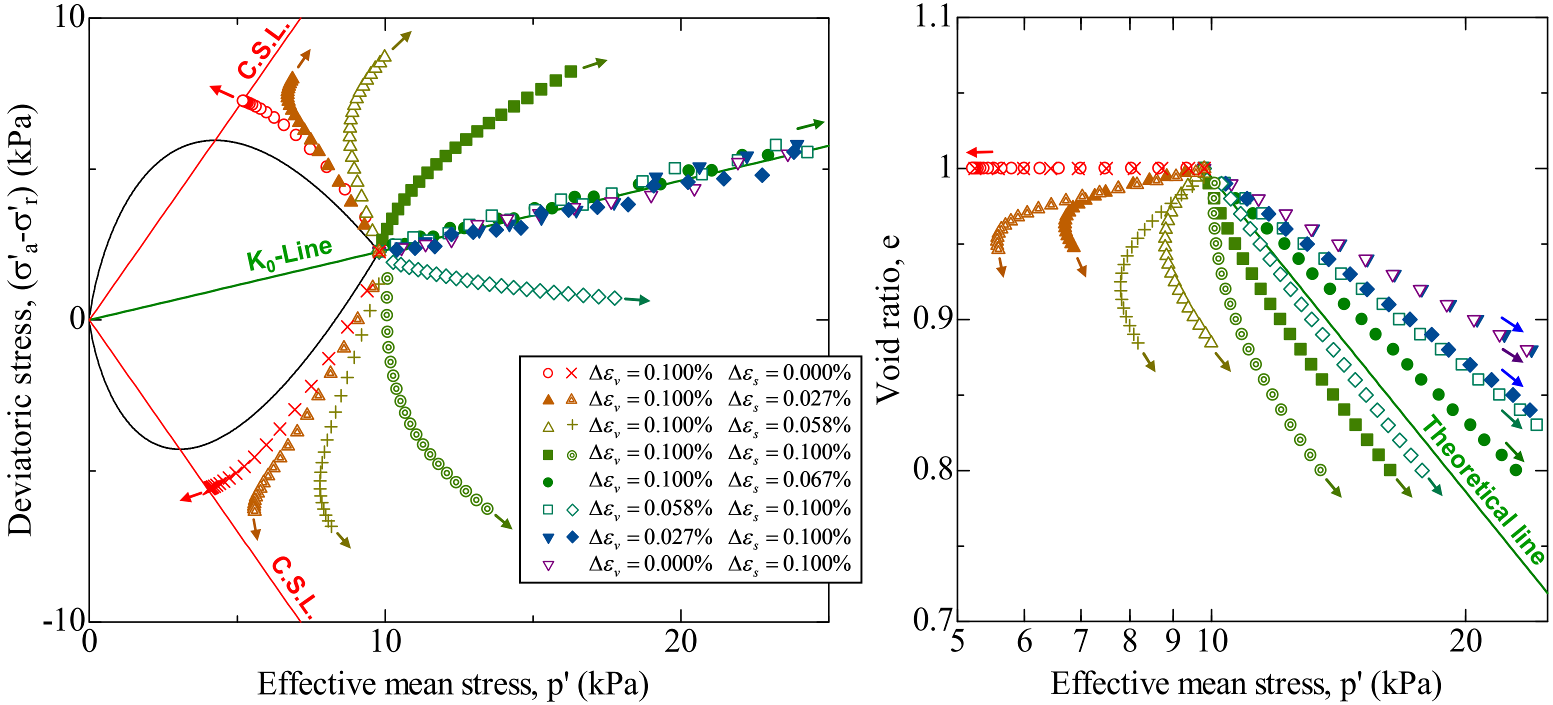

(a) Effective stress path

(b) e-lnp' relation

Fig 2.3 Simulation result of effective stress path and e-lnp' relation near to singular point on the yielding surface of SO model before coping the singular point

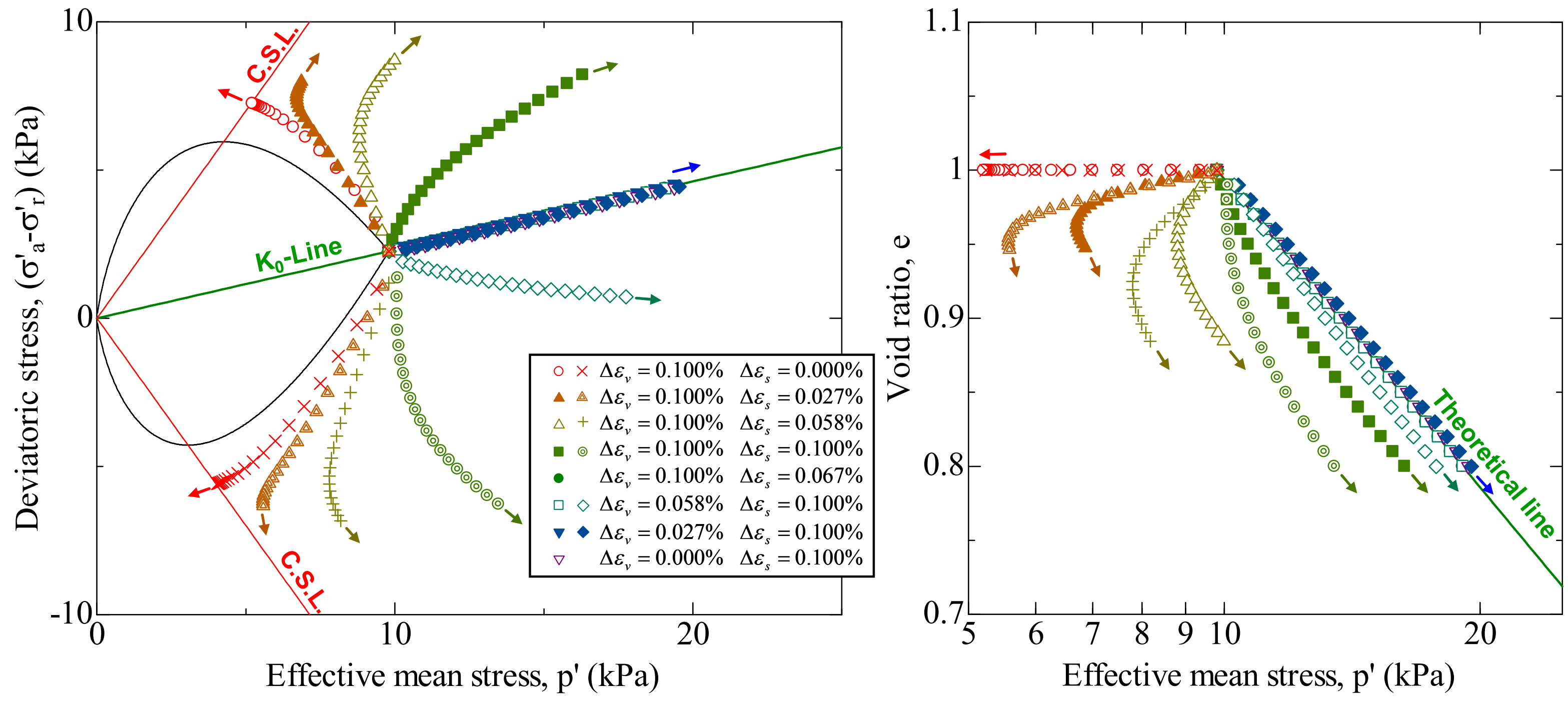

(a) Effective stress path **(b) e-lnp' relation**

Fig 2.4 Simulation result of effective stress path and e-lnp' relation near to singular point on the yielding surface of SO model after coping the singular point

2-Details of theories used in DACSAR

1. Constitutive models employed in DACSAR
2. Singular point on the yielding surface (SO)
3. Yielding Judgment
4. Metastability (SO-EP)
5. Functions
6. Macro element proposed by Sekiguchi et al.
7. Bar, Beam, shell element etc.

3. Yielding Judgment
(Takeyama,2007, Doctoral dissertation)

3.1 Improved Yielding judgment criterion for SO-EVP, EC-EVP, LC-EVP model

3.2 Corrected Akai & Tamura's method for spatially discretization of pore water dissipation

3.3 1D consolidation (coupled) for Linearly elastic body by using two types of mesh generations

Improved judgment criterion

(1) For elastic state

$$\begin{cases} g(\sigma', h) = f(\sigma') - h < 0: & \text{elastic} \\ g(\sigma', h) = f(\sigma') - h \geq 0: & \text{elasto - visco - plastic} \end{cases}$$

(2) For elasto-visco-plastic state

$$\begin{cases} \gamma < 0: & \text{elastic} \\ \gamma \geq 0: & \text{elasto - visco - plastic} \end{cases}$$

For SO-EVP $$f = MD\ln\frac{p'}{p'_0} + D\cdot\eta *,$$

For EC-EVP $$f = MD\ln\frac{p'}{p'_0} + \frac{MD}{n_E}\cdot\left(\frac{\eta *}{M}\right)^{n_E}$$

For LC-EVP $$f = MD\ln\frac{p'}{p'_0} + \frac{2MD}{n_L}\cdot\ln\left[1+\left(\frac{\eta *}{M}\right)^{n_L}\right]$$

$$g(\sigma', h) = f(\sigma') - h = 0$$

$$h(\varepsilon_v^{\mathrm{p}}, t) = \alpha\cdot\ln\left\{\frac{\alpha}{\dot{v}_0 t}\left[\exp\left(\frac{\varepsilon_v^{\mathrm{vp}}}{\alpha}\right) - 1\right]\right\}$$

$$\gamma = -\frac{\dfrac{\partial F}{\partial \sigma'} : \mathrm{C^e} : \dot{\varepsilon} + \dfrac{\partial F}{\partial t}}{\dfrac{\partial F}{\partial \sigma'} : \mathrm{C^e} : \dfrac{\partial F}{\partial \sigma'} - \dfrac{\partial F}{\partial \varepsilon_v^{\mathrm{vp}}}\dfrac{\partial F}{\partial p'}}$$, is plastic coefficient, $\dot{\varepsilon}_v^{\mathrm{vp}} = \gamma\dfrac{\partial F}{\partial p'}$

Yielding judgment criterion for SO model at the singular point

(1) The stress proceeds on the singular point(figure 1(a))

$$\begin{cases} \dot{\gamma}_1 > 0 \\ \dot{\gamma}_2 > 0 \end{cases} \quad \longrightarrow \quad \dot{\varepsilon}^{\mathrm{p}} = \dot{\gamma}_1 \frac{\partial f_1}{\partial \sigma'} + \dot{\gamma}_2 \frac{\partial f_2}{\partial \sigma'}$$

(2) The stress gets away from the singular point(figure 1(b))

$$\begin{cases} \dot{\gamma}_1 > 0 \\ \dot{\gamma}_2 \leq 0 \end{cases} \quad \longrightarrow \quad \dot{\varepsilon}^{\mathrm{p}} = \dot{\gamma}_1 \frac{\partial f_1}{\partial \sigma'}$$

$$\begin{cases} \dot{\gamma}_1 \leq 0 \\ \dot{\gamma}_2 > 0 \end{cases} \quad \longrightarrow \quad \dot{\varepsilon}^{\mathrm{p}} = \dot{\gamma}_2 \frac{\partial f_2}{\partial \sigma'}$$

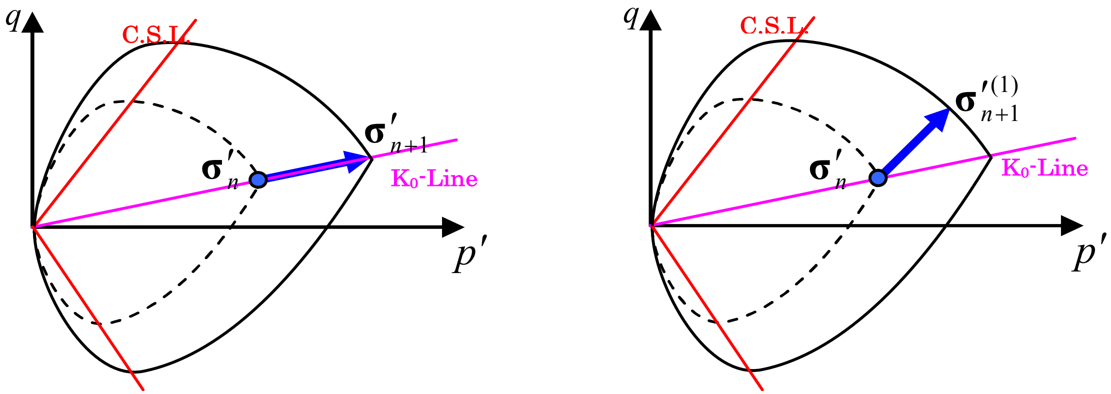

(a) Stress proceeds on the singular point

(b) Stress gets away from the singular point

Fig.3.1

$$\begin{Bmatrix} \dot{\gamma}_1 \\ \dot{\gamma}_2 \end{Bmatrix} = \frac{1}{\det X} \begin{bmatrix} X_{22} & -X_{12} \\ -X_{21} & X_{11} \end{bmatrix} \begin{Bmatrix} L_1 \\ L_2 \end{Bmatrix}$$

where, $\det X = X_{11}X_{22} - X_{12}X_{21}$

$$X_{11} = \frac{D^2}{p'^2}\left(\beta_1{}^2 K + 3G + \frac{p'}{D}\beta_1 \right), \quad X_{12} = \frac{D^2}{p'^2}\left(\beta_1\beta_2 K - 3G + \frac{p'}{D}\beta_2 \right)$$

$$X_{21} = \frac{D^2}{p'^2}\left(\beta_1\beta_2 K - 3G + \frac{p'}{D}\beta_1 \right), \quad X_{22} = \frac{D^2}{p'^2}\left(\beta_2{}^2 K + 3G + \frac{p'}{D}\beta_2 \right)$$

$$\beta_1 = \mathrm{M}\text{-}\sqrt{\frac{3}{2}}\left(\eta_0 : \overline{n}_v\right), \beta_2 = \mathrm{M}\text{-}\sqrt{\frac{3}{2}}\left(\eta_0 : \overline{n}_v\right), \overline{n}_v = \frac{(1-\Lambda)K\dot{\varepsilon}_v\eta_0 - 2G\dot{\varepsilon}_d}{\left\|(1-\Lambda)K\dot{\varepsilon}_v\eta_0 - 2G\dot{\varepsilon}_d\right\|}$$

3.2 Corrected Akai & Tamura's method

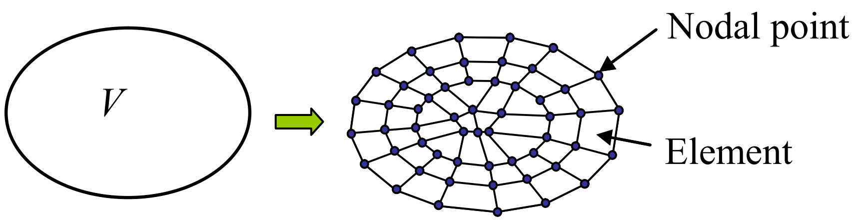

Quadrangular divided

Fig 3.2 spatial discretization

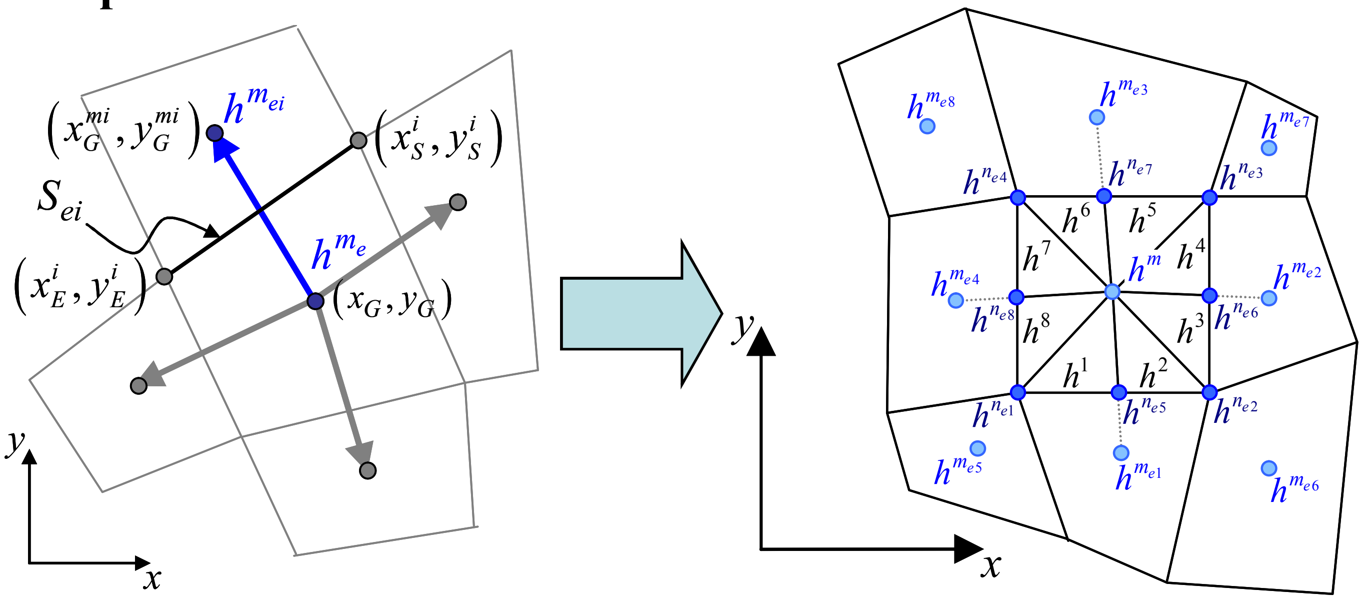

(a) original method **(b) corrected method**

Fig3.3 Method for Spatially discretization of pore water dissipation (consolidation) be corrected

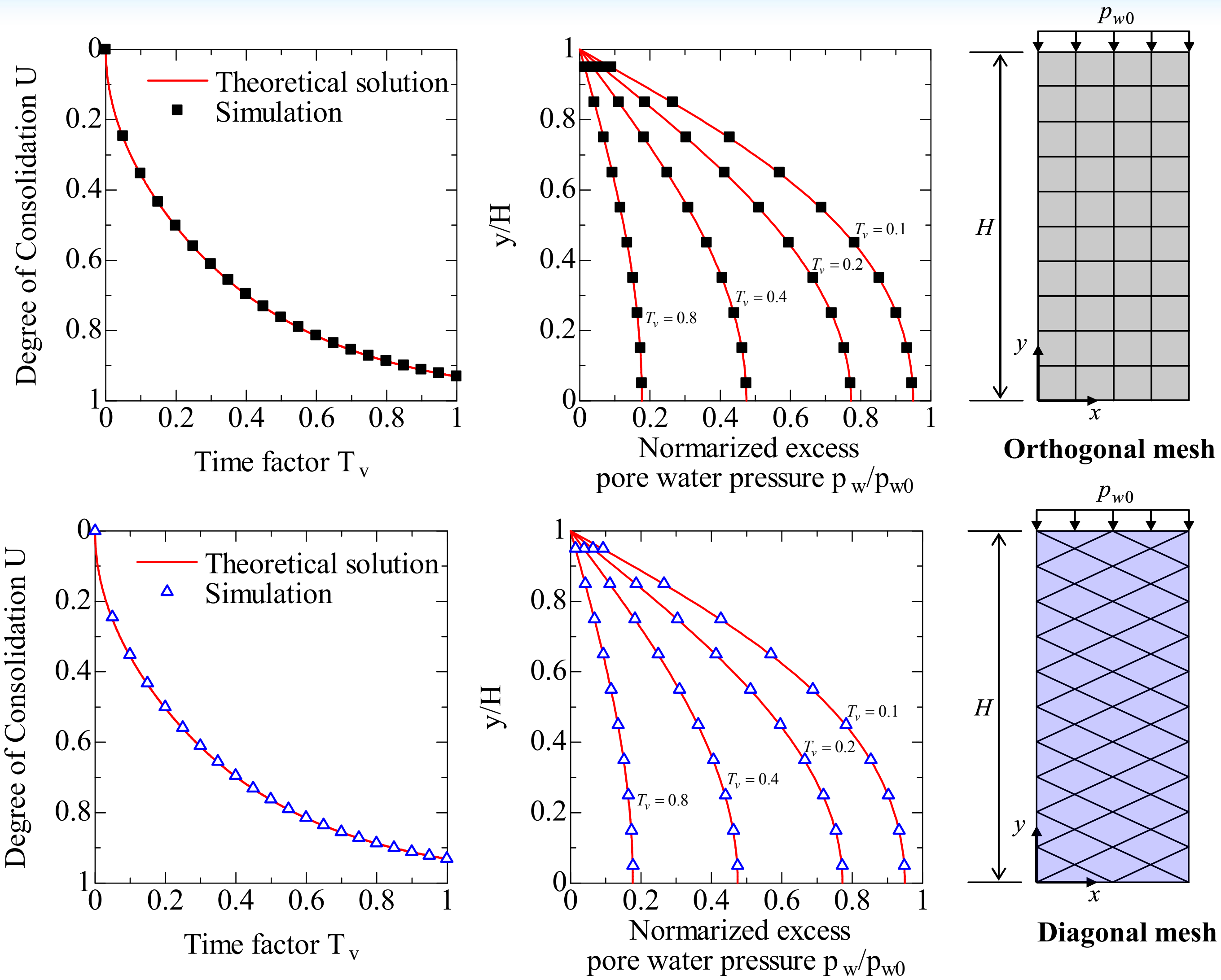

Fig3.4 Simulation of 1-D consolidation by using two types of mesh

2-Details of theories used in DACSAR

1. **Constitutive models employed in DACSAR**
2. **Singular point on the yielding surface (SO)**
3. **Yielding Judgment**
4. **Metastability (SO-EP)**
5. **Functions**
6. **Macro element proposed by Sekiguchi et al.**
7. **Bar, Beam, shell element etc.**

4. Metastability (SO-EP)

(Takeyama,2007, Doctoral dissertation)

4.1 Theoretical explanation

4.2 Demonstration

For the isotropic consolidated clay, the infinitesimal increment of stress ratio can induce a rapid plastic shear deformation, which is called Metastability characteristic (Roscoe et.al. 1963), this stress state can be called Metastable state.

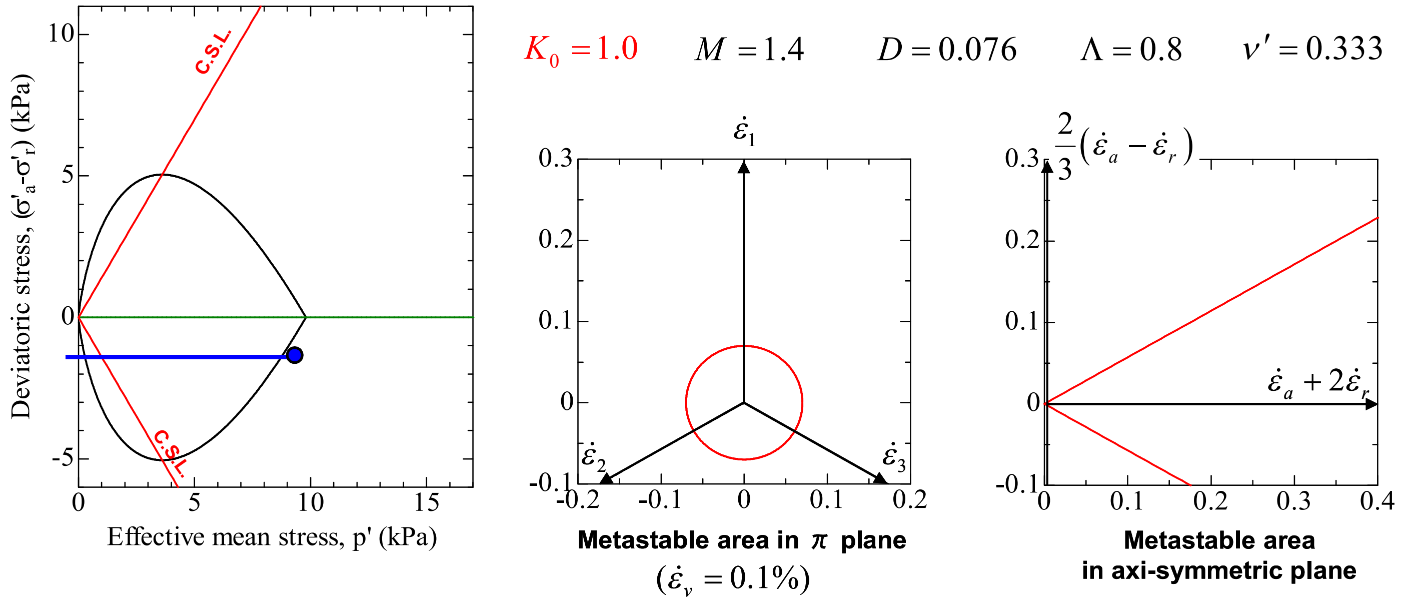

Fig4.1 Metastable area

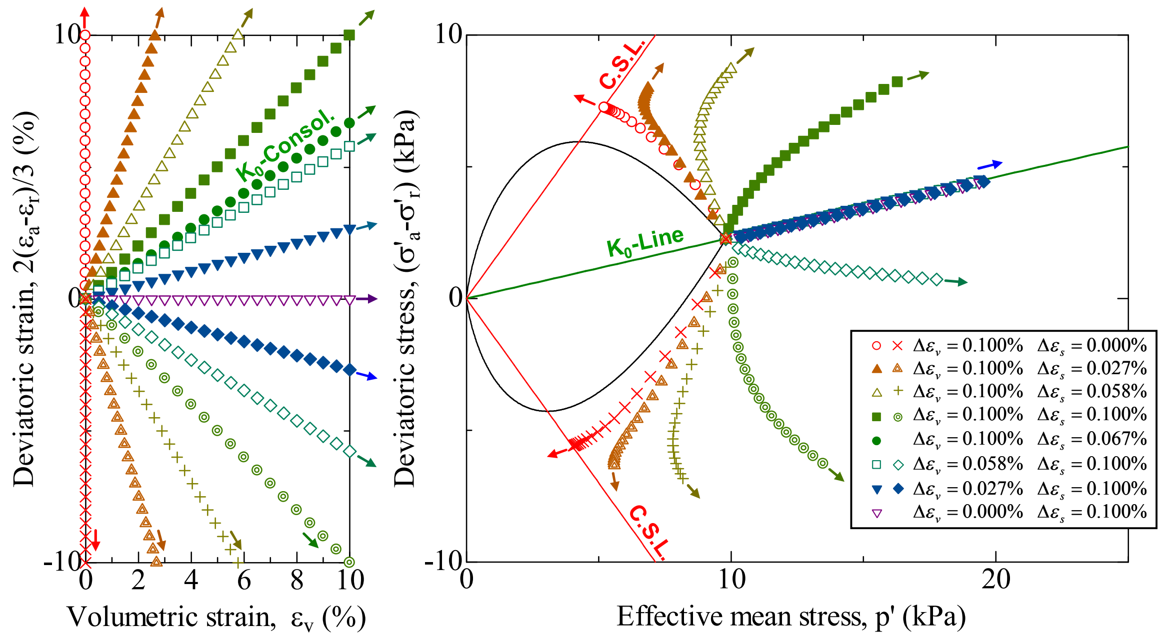

Fig4.2 Simulation results of effective stress path according to given strain path for the metastable area of SO model after coping the singular point

2-Details of theories used in DACSAR

1. Constitutive models employed in DACSAR

2. Singular point on the yielding surface (SO)

3. Yielding Judgment

4. Metastability (SO-EP)

5. Functions

6. Macro element proposed by Sekiguchi et al.

7. Bar, Beam, shell element etc.

5. Functions

In DACSAR program, the numerical solution of initial boundary-value problem relies on the finite element method (FEM) based on spatial and time discretization. For the numerical integration procedures, the integration of constitutive equation over a time step to calculate the stress and strain changes corresponding to the change of the displacement is accomplished by using the algorithm to solve the systems of linear equations.

Systems of linear equations on the relation between nodal force and nodal dispalacement

$$\Delta \mathrm{F} = \mathrm{K} \cdot \delta \mathrm{d}$$

where, $\mathrm{K} = \sum_{e} \int_{\Omega^{e}} \mathrm{B}_{e}^{T} \mathrm{C}^{ep} \mathrm{B}_{e} d\Omega^{e}$, is total stiffness matrix,

$\mathrm{B}_{e} = \mathrm{LN}$, is strain matrix, L is differential operator for plain problem,

N is shape function

5. Functions

The integration technique adopted can be classified into
explicit method: Gaussian method
implicit method: Biconjugate gradient stabilized method and

5.1 Simple explicit method

5.2 Implicit (iterative) calculation method

5.1 Simple explicit method

Total stiffness equations

$$\mathrm{K} \cdot \delta \mathrm{d} = \Delta \mathrm{F}$$

$$\Downarrow$$

Forward elimination process

$$\mathrm{L}_{n\text{-}1}^{-1}\mathrm{L}_{n\text{-}2}^{-1} \cdots\cdots \mathrm{L}_{2}^{-1}\mathrm{L}_{1}^{-1}\mathrm{K} = \mathrm{K}^{(n-1)} \qquad \mathrm{L}_{n\text{-}1}^{-1}\mathrm{L}_{n\text{-}2}^{-1} \cdots\cdots \mathrm{L}_{2}^{-1}\mathrm{L}_{1}^{-1}\delta\mathrm{F} = \delta\mathrm{F}^{(n-1)}$$

$$\Downarrow$$

Backward substitution process

$$\delta d_n = \frac{\delta F_n^{(n-1)}}{K_{nn}^{(n-1)}}$$

$$\delta d_i = \left(\delta F_i^{(n-1)} - \sum_{j=i+1}^{n} K_{ij}^{(n-1)} \delta d_j \right) \Big/ K_{ii}^{(n-1)}$$

Fig5.1 Calculation process of Gaussian method

Implicit (iterative) calculation method (BiCGSTAB)

Algorithm procedure

Allocate temporary vectors $p, \hat{p}, s, \hat{s}, t, v, \tilde{r}$
Allocate temporary reals $r_1, r_2, \alpha, \beta, \omega$

$r := \Delta F - K \cdot \delta d$
$\tilde{r} = r$

For i:=1 step 1 until max_itr do

- $r_1 = \tilde{r} \cdot r$
- If i = 1 then $p := r$ else
- $\beta = (r_1 / r_2) * (\alpha / \omega)$
- $p = r + \beta * (p - \omega * v)$
- End if
- Solve ($M \cdot \hat{p} = p$)
- $v = K \hat{p}$
- $\alpha = r_1 / (\tilde{r} \cdot v)$
- $s = r - \alpha \cdot v$
- Solve ($M \cdot \hat{s} = s$)
- $t = K \cdot \hat{s}$
- $\omega = (t \cdot s)/(t \cdot t)$
- $x = x + \alpha \cdot \hat{p} + \omega \cdot \hat{s}$
- $r = s - \omega * t$
- $r_2 = r_1$

End (i-loop)

Deal locate all temp memory
Return TRUE

2-Details of theories used in DACSAR

1. **Constitutive models employed in DACSAR**
2. **Singular point on the yielding surface (SO)**
3. **Yielding Judgment**
4. **Metastability (SO-EP)**
5. **Functions**
6. **Macro element proposed by Sekiguchi et al.**
7. **Bar, Beam, shell element etc.**

6. Macro element proposed by Sekiguchi, Shibata, Mimura, Sumikura(1988)

6.1 Explanation of the macro element

6.2 Explanation of input parameters
for the macro element

6.3 Demonstration

- Macro element is a big physical domain which includes foundation area and vertical drain in this area.

- Macro element method is used to predict the post-construction stress changing and deformation, especially for the plane strain problem of vertical drain casting by using the construction method such as SCP / SD/CVC

- The constitutive model of SO, linear elastic, modified cam-clay, EC and LC can be used.

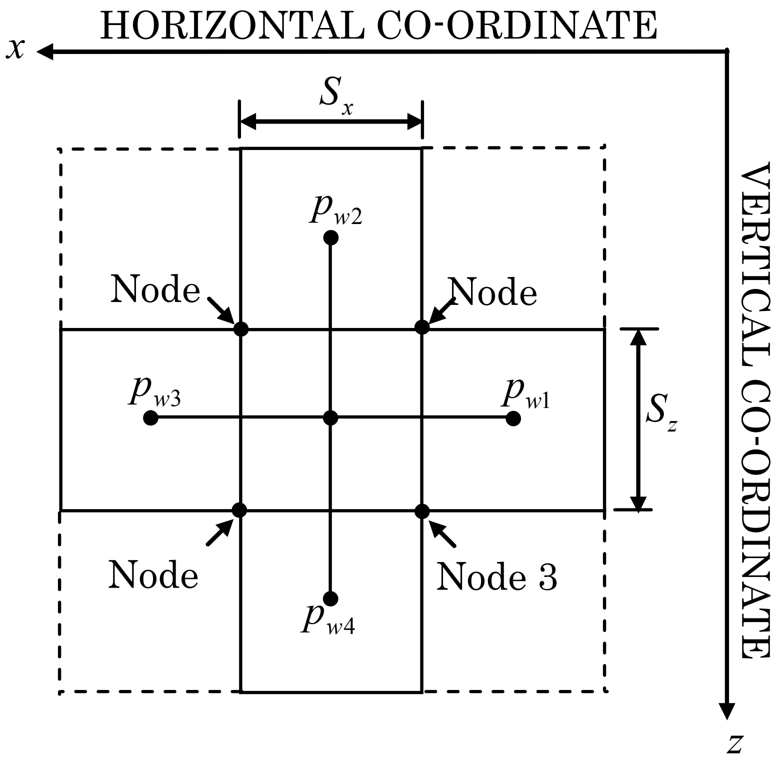

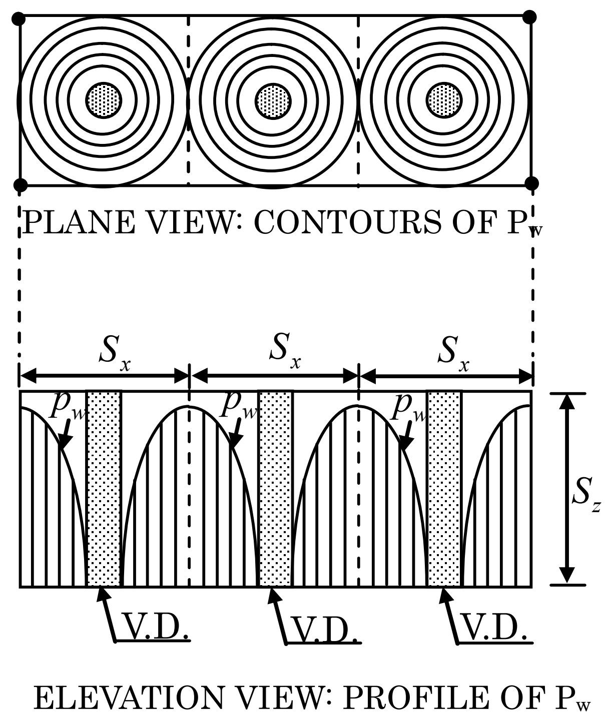

Fig6.1 Sketch showing the freedom of excess pore water of a centered macro element and those of the adjoining four elements

Fig6.2 Sketch illustrating the distribution of excess pore water pressures around equally spaced vertical drains

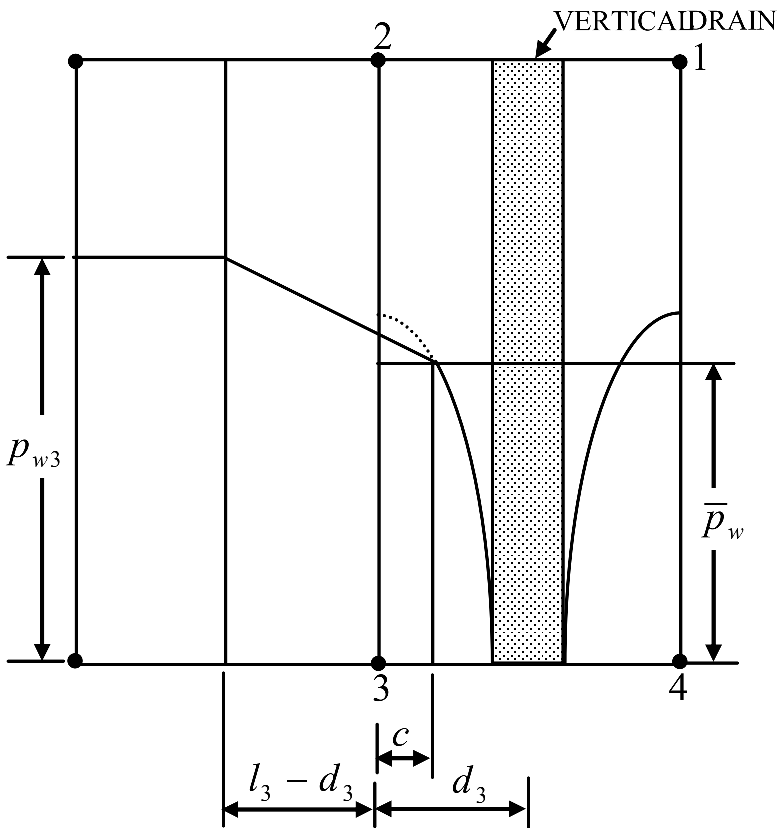

Fig6.3 Sketch illustrating the proposed way of considering water flow across the boundary between the treated and untreated regions

- ✓ **Model parameters**
- ✓ **Radius of drain**
- ✓ **Effective collector radius**
- ✓ **Boundary condition**

Material parameters for macro element

$\tilde{\lambda}$ (kN/m^2)	$\tilde{\mu}$ (kN/m^2)	σ'_{vi} (kPa)	K_i	k (m/day)
1.338	667	9.8	0.65	8.64*10^{-5}

Three kinds of cases

Case	$S_x (= S_y)$(m)	S_z (m)	a (m)	b (m)
1	2.0	1.0	0.2	1.12838
2	1.0	1.0	0.1	0.56419
3	1.0	2.0	0.1	0.56419

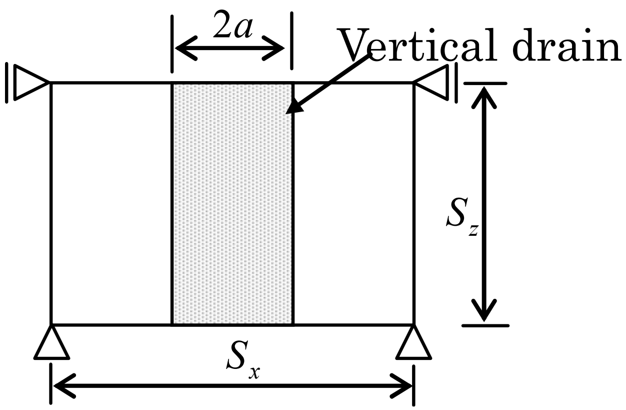

Fig6.4 Macro element model with a vertical drain

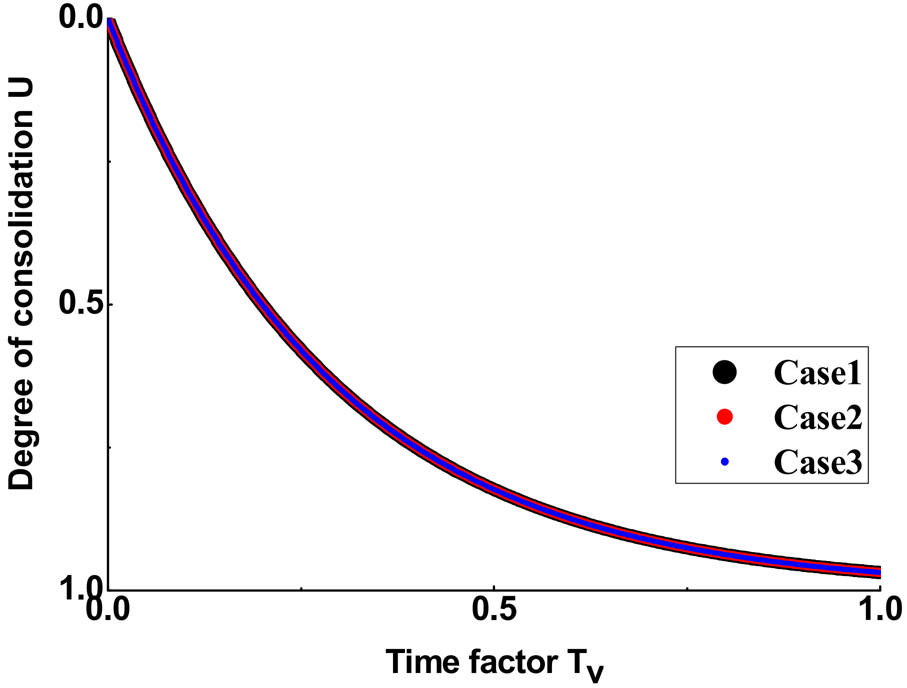

Fig6.5 Relation between degree of consolidation and time factor for macro element

2-Details of theories used in DACSAR

1. Constitutive models employed in DACSAR
2. Singular point on the yielding surface (SO)
3. Yielding Judgment
4. Metastability (SO-EP)
5. Functions
6. Macro element proposed by Sekiguchi et al.
7. Bar, Beam, Joint, Shell element

7. Bar, Beam, shell element etc.

MT	Element type	Application element is used to represent
2	Linearly elastic Beam element	1. Flexural members in a building frame 2. Columns in a building frame 3. Sheet pile walls
3	Linearly elastic Bar element	1. Reinforcement in reinforced earth structures 2. Tie backs for anchor walls 3. Springs 4. Structural Braces/Struts
4	Elastic perfectly plastic Joint element	1. Interface between soil and rock 2. Interface between fill and concrete retaining wall 3. Interface between soil and reinforcement in reinforced earth structures 4. Rock joints/fractures
5	Linearly plastic Shell element	Supporting structure in the ground
7	Hyperbolic plane element	1. Saturated soil inducing fills and foundation 2. Mass concrete structure 3. Rock

CONTENTS

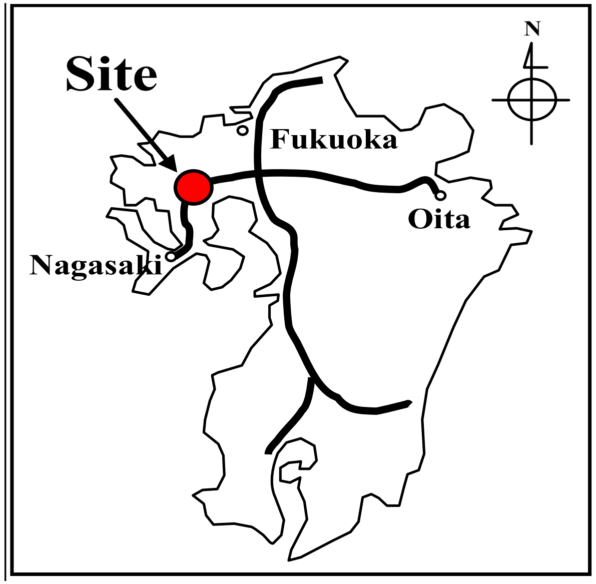

Fig.3-1 Embankment as cycle way in north of Takeo I.C

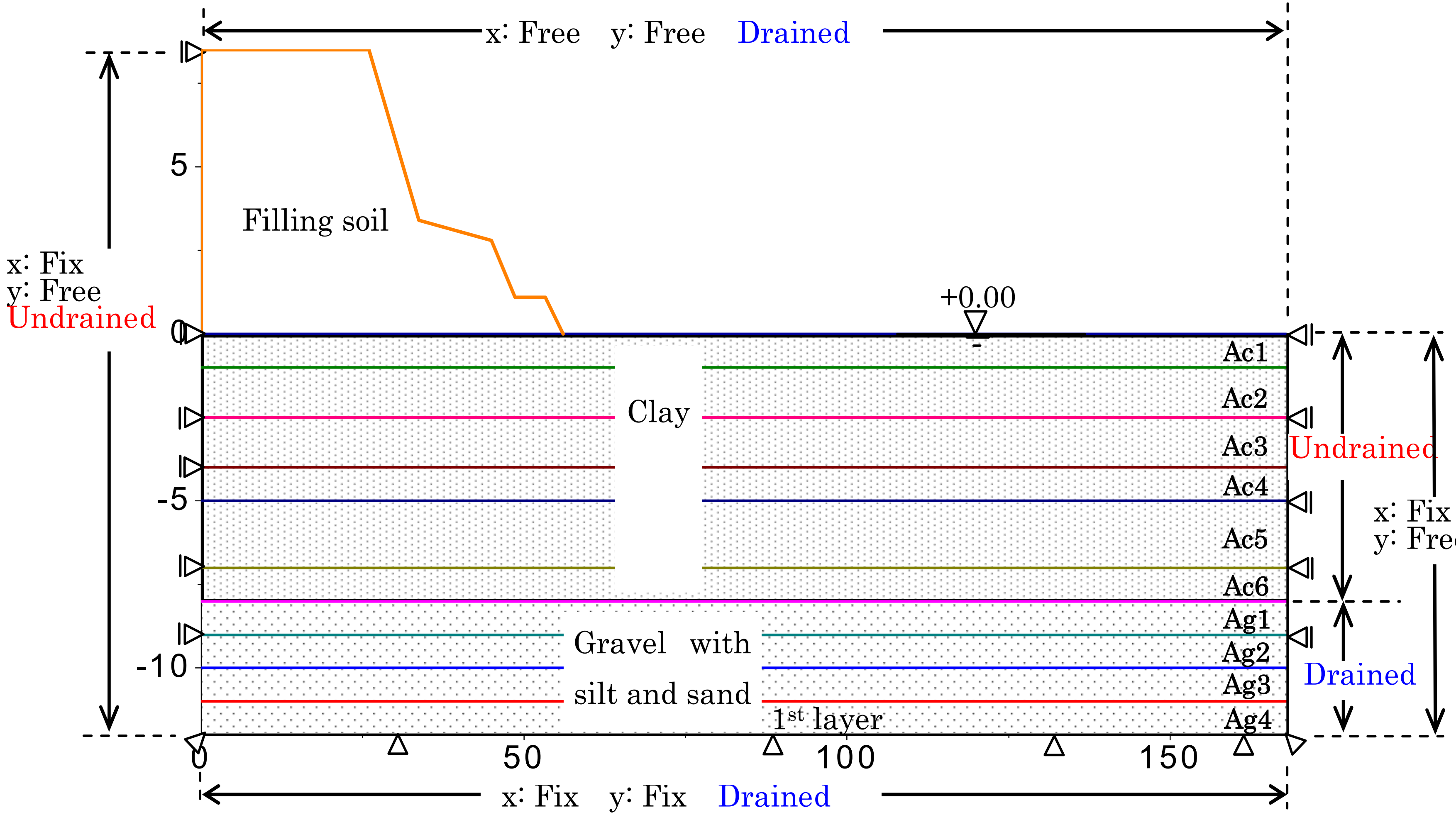

Fig.3-2 Sketch for one typical part of the embankment with its foundation and the boundary conditions

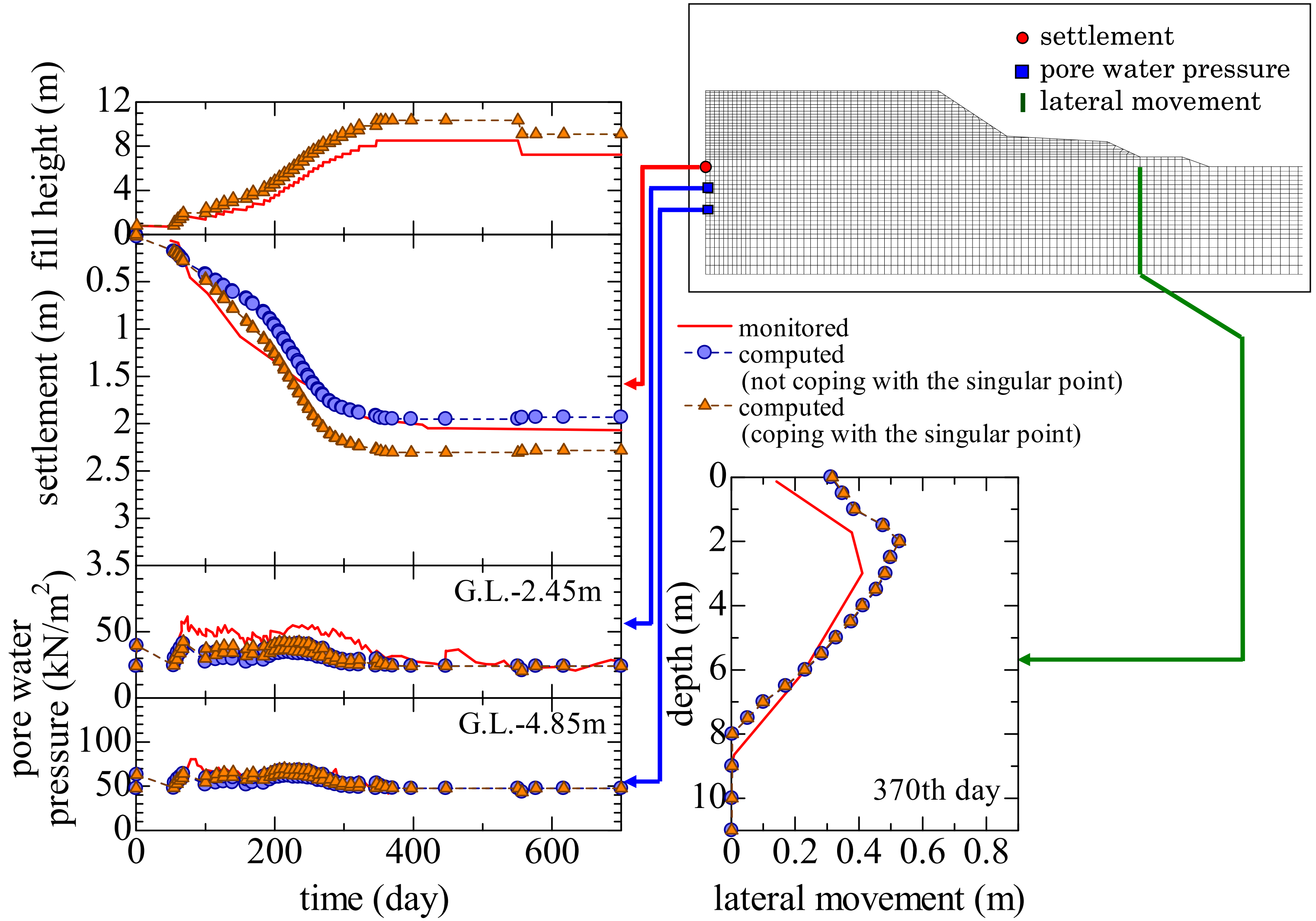

Fig.3-3 Monitored and Simulation results

THANKS FOR

YOUR ATTENTION